12 Remote Sensing of Rangeland Biodiversity

E. Raymond Hunt Jr., Cuizhen Wang, D. Terrance Booth, Samuel E. Cox, Lalit Kumar, and Matthew Reeves

ACRONYMS AND DEFINITIONS

ASTER	Advanced Spaceborne Thermal Emission and Reflection Radiometer
ETM+	Enhanced Thematic Mapper Plus
EVI	Enhanced Vegetation Index
GIS	Geographic Information System
IKONOS	A commercial Earth observation satellite, typically, collecting sub-meter to 5 m data
ISODATA	Iterative Self-Organizing Data Analysis Technique
LiDAR	Light Detection and Ranging
MERIS	Medium Resolution Imaging Spectrometer
MODIS	Moderate-Resolution Imaging Spectroradiometer
NASA	National Aeronautics and Space Administration
NDVI	Normalized Difference Vegetation Index
NIR	Near-Infrared
NOAA	National Oceanic and Atmospheric Administration
OLI	Operational Land Imager
PROSAIL	Combination of PROSPECT and SAIL, the two nondestructive physically based models to measure biophysical and biochemical properties
PROSPECT	Radiative transfer model to measure leaf optical properties spectra
SAIL	Scattering by Arbitrary Inclined Leaves
SAVI	Soil Adjusted Vegetation Index
SVM	Support Vector Machines
SWIR	Shortwave Infrared
TM	Thematic Mapper
UAS	Unmanned Aircraft Systems
USDA	United States Department of Agriculture
VIIRS	Visible Infrared Imaging Radiometer Suite

12.1 INTRODUCTION

Rangelands are a type of land cover dominated by grasses, grass-like plants, broadleaf herbaceous plants (forbs), shrubs, and isolated trees, usually in which large herbivores evolved as part of the ecosystem. In many rangelands, the large herbivores were replaced by livestock, and thus livestock grazing represents a major land use for production of food and fiber. Sustainability is maintained by species diversity (Kouba et al., 2024; Retallack et al., 2023; Hooper et al., 2005; Tilman et al., 2006, 2012; Zaveleta et al., 2010; Reich et al., 2012) and reduction of biodiversity is expected to be one of the major consequences of global climatic change (Soussanna and Lüscher, 2007; Janetos et al., 2008; McKeon et al., 2009; Pereira et al., 2010, 2012; Belgacem and Louhaichi, 2013; Joyce et al., 2013; Polley et al., 2013). Along with climatic change, invasions of

DOI: 10.1201/9781003541165-15

non-native species are threatening rangeland sustainability by decreasing native species diversity (Retallack et al., 2023; Thornley et al., 2023; Matongera et al., 2021; Sawalhah et al., 2018; Jafari et al., 2017; McCord et al., 2017; Bradley et al., 2009; Lavergne et al., 2010; Ziska et al., 2011).

Rangelands cover large, sparsely populated areas; thus, remote sensing is becoming much more important for rangeland monitoring, whether the objectives are sustainable livestock foraging or maintenance of other ecosystem goods and services with climatic change. Different stakeholders at the national, state/province, and landscape scales have different needs, which may require remotely sensed data at different spatial, temporal or spectral resolutions. Reeves et al. (Chapter 11 of this volume) examined the relationship between rangeland productivity and climate, which highlights some of the direct mechanisms on how rangelands may respond to increased atmospheric CO_2, global warming, and changes in precipitation regimes. Methods and techniques of rangeland characterization using remote sensing are covered by Kumar et al. (Chapter 12 of this volume).

Monitoring the biodiversity of rangelands is critical for maintaining sustainability; therefore, one of the major challenges for remote sensing is how to use imagery to estimate biodiversity (Kouba et al., 2024; Ocholla et al., 2024; Fenetahun et al., 2022; Matongera et al., 2021; Sawalhah et al., 2018; Jafari et al., 2017; McCord et al., 2017; Ludwig et al., 2004; John et al., 2008; Gillespie et al., 2008; Huang and Asner, 2009; Ward and Kutt, 2009). Diversity of plant functional types (PFTs) may be a good indicator of biodiversity, and determining the diversity of PFTs by remote sensing may be easier than determining plant species richness (Ustin and Gamon, 2010). However, land-cover and land-use maps based on global-scale PFTs (Running et al., 1995; Friedl et al., 2010) do not provide sufficient information for conserving and managing rangelands.

This chapter examines data types and methods for remote sensing of biodiversity at different resolutions: spectral, temporal and spatial. Medium resolution sensors, such as the Landsat 8 Operational Line Imager (OLI), generally have resolutions on the order of 10–60 m, 10–20 days, and 4–10 bands for spatial, temporal and spectral resolutions, respectively. High spectral resolution (hyperspectral) sensors generally have 100 or more contiguous bands, which are used to determine a reflectance spectrum of the land surface. High temporal resolution is usually provided by satellites, such as the MODerate resolution Imaging Spectroradiometer (MODIS), that have a broad swath (>400 km) in order to cover the Earth frequently. Commercial vendors provide satellite data with panchromatic bands of about 0.5 m and multispectral bands of about 2–3 m spatial resolution, but for this chapter, high spatial resolution (HSR) data have pixel sizes of 10 cm or less, and are acquired by aircraft or ground-based imaging.

To be useful for rangeland managers, remote sensing data must be able to estimate biodiversity at a landscape scale, and the information must be compatible with rangeland management systems based on ecological sites, rangeland state-and-transition models, and rangeland health. With over 40 years of data acquired from the Landsat satellites, and extensive programs of research, Landsat imagery have not been used routinely to provide information necessary to affect managers' decisions on which land areas are used for a given purpose at a given time. Remote sensing data providers and analysts must adapt to the needs of rangeland managers, and the needs are increasingly being driven by issues of sustainability, based on maintaining biodiversity. Therefore, we briefly describe rangeland management concepts and then describe remote sensing data and methods related to rangeland biodiversity. From this perspective, we conclude that HSR data acquired from aircraft provide the necessary data and will have the highest impact on management decisions. However, HSR data have their own unique challenges.

12.2 BIODIVERSITY AND RANGELAND MANAGEMENT

A plant community is a set of interacting species co-occurring at a given site, with dominant species identified by mass and typical longevity of an individual. Management of U.S.

rangelands was built on Clements' (1916) theory of plant succession where the dominant plant species changed over time to a set of species in equilibrium with climate, which is defined as the climax plant community (Brown, 2010). These communities were assumed to have the highest sustainable productivity and greatest resistance to invasive species. Overgrazing was assumed to reverse the plant community to an earlier stage of succession (Sampson, 1919). For monitoring and management, rangeland sites were defined by assuming the climax plant community was the dominant plant community at the onset of European immigration and settlement into the Western United States.

However, it was recognized that with natural disturbances such as fire, drought and grazing, plant succession was much more dynamic and variable. Furthermore, after severe overgrazing and soil erosion, it was unlikely that the climax community could re-establish itself without costly interventions. In response to the deficiencies of Clementsian succession, two ideas emerged in parallel (Briske et al., 2005): state-and-transition models (Brown, 1994, 2010), and rangeland health (NRC, 1994). To better guide range management based on these two ideas, the concept of rangeland sites was replaced with the concept of ecological sites in which the various plant communities are in a dynamic equilibrium determined by the natural disturbance regime.

12.2.1 Ecological Sites and State-and-Transition Models

> *An ecological site is a conceptual division of the landscape, defined as a distinctive kind of land based on recurring soil, landform, geological, and climate characteristics that differs from other kinds of land in its ability to produce distinctive kinds and amounts of vegetation and in its ability to respond similarly to management actions and natural disturbances.*
>
> *(Caudle et al., 2013)*

In the U.S., the top-levels of a hierarchical classification system based on soil, landform, geology, and climate are the Land Resource Region (LRR) and Major Land Resource Area (MLRA), defined by the USDA NRCS (2006). Subdividing MRLAs based on finer scale differences in climate, geomorphology and soils, the next level down in the hierarchy is the Land Resource Unit (LRU), LLRs, MLRAs, LRUs, and ecological sites are provisional and may be revised with more information (Moseley et al., 2010; Caudle et al., 2013). In a MRLA or LRU, ecological sites are identified by a reference state (State 1) and reference plant community (Community Phase 1.1), based on the dominant vegetation thought to be present at the time of European immigration and settlement (Figure 12.1). Ecological sites are divided into a series of alternative states (States 2, 3 . . . to some number *N*), which recognize new sets of stable communities that become self-perpetuating (Figure 12.1). Land areas in most alternative states are not barren wastes; with appropriate management, these areas may be used sustainably by preventing further degradation.

The definition of an ecological site raises an important drawback for remote sensing – the reference plant community is usually inferred from a wide variety of sources, and mapped using geographic information data. An ecological site is not defined by the plant community that is currently occupying it; therefore, remotely sensed land cover, at any resolution, cannot be used to define an ecological site. Whereas ecological sites are not defined by the plant communities, ecological states may be mapped using characteristic plant communities determined from high-resolution aerial photographs (Steele et al., 2012).

Within an ecological state (for example, Reference State 1, Figure 12.1), various plant community phases result from natural disturbances (including grazing by livestock) and subsequent plant succession leads back to the reference community phase (Figure 12.1). Together, all of the community phases in Reference State 1 represent the natural range of variation found over time (Caudle et al., 2013). Land areas in Community Phases 1.2, 1.3, and 1.4 are not considered degraded simply because the plant community is not in Phase 1.1, even though there may be fewer species and less biomass. Change detection must distinguish between changes within a state compared to a change of state. For example, there is less foliar mass in grasslands either after a drought (a frequent occurrence within the range of natural variability) or after severe overgrazing by livestock (which frequently entails a state change; Stafford Smith et al., 2007). Demonstrating a change with remote sensing is not a demonstration that a state-change has occurred (Thornley et al., 2023; Matongera et al., 2021; Sawalhah et al., 2018; Jafari et al., 2017; McCord et al., 2017 (Bastin et al., 2012; Bradley, 2013).

State-and-transition models are provisional hypotheses that describe the ecological processes leading to transitions (T1.A, T1.B, Figure 12.1) from one state to another (Caudle et al., 2013).

For example, invasion of downy brome (*Bromus tectorum* L.) into Great Basin sagebrush ecosystems increased the frequency of fire, which enhanced the dominance of downy brome in a feedback loop (Balch et al., 2013).

Thresholds are the conceptual boundaries dividing alternative states which are crossed during transitions (Briske et al., 2005, 2006; Bestelmeyer, 2006). Ecological resilience describes how much disturbance an ecological site can withstand without crossing a threshold into an alternative state; operationally, resilience may be defined as multiple species having the same ecological function (Questad et al., 2022; McCord et al., 2017; Elmqvist et al., 2003; Folke et al., 2004; Allen et al., 2005; Briske et al., 2008). For most stakeholders, the goal for monitoring rangelands is to determine if an ecological site is in the process of transitioning to alternative state. These transitions are not distributed evenly over an area or over time, so monitoring plant communities requires a larger and longer perspective (Bestelmeyer et al., 2011; Williamson et al., 2012). Determining the amount of species diversity, or at least an array of PFTs, is a primary objective for developing science-based, cost-effective tools for rangeland monitoring based on remote sensing.

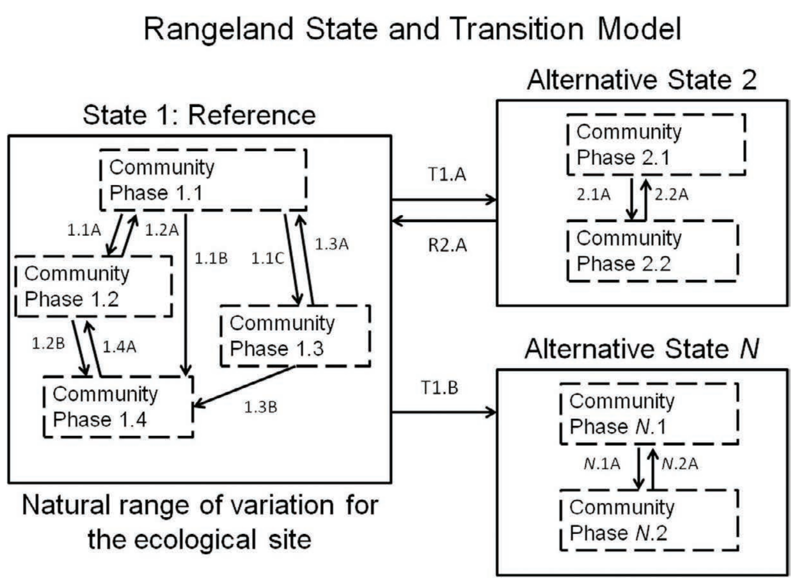

FIGURE 12.1 State-and-transition model for an ecological site in the USA. Outer boxes (solid lines) represent stable ecological states (A, B, . . . , *N*) within which changes in community phases (dashed lines) result from natural disturbances and succession (arrows). State 1 is the reference state and community phase 1 represents the historic climax plant community. Other community phases represent the range of natural variation and may be identified by dominant plant species. Transitions from one state to another stable state occur when a threshold is crossed (bold arrows), which is usually irreversible without intensive inputs.

12.2.2 Biodiversity Metrics for Managing Australian Rangelands

Rangelands, including tropical savannas, woodlands, shrublands and grasslands, make up 75% of Australia, with 55% of these rangelands being grazed by livestock. The Australian Collaborative Rangelands Information System (ACRIS) was set up in 2002 to support the Commonwealth and state governments in better managing the rangelands (Bastin et al., 2009; Eyre et al., 2011a; Oliver et al., 2014). In Australia, each state has its own regulations and methods of assessing and managing rangelands, and ACRIS is the overarching body that supports this by collating and synthesizing the monitoring data and making these data available to interested parties. This information assists natural resource management organizations, state governments, and the commonwealth in planning and reporting obligations, and evaluating the effectiveness of investments.

For determining the health, condition and biodiversity of rangelands, extensive surveys on a repeated basis are essential. Surveys of species presence and abundance are time consuming and expensive if undertaken at broad scales. For rapid monitoring, three states developed multi-metrics for biodiversity to help in the assessment of site conditions:

(1) BioCondition (in Queensland),
(2) Habitat Hectares (in Victoria), and
(3) BioMetric (in New South Wales).

BioCondition is a vegetation and biodiversity assessment framework developed by the Queensland Department of Resource Management to provide on-site guidance to beginners and document the assessment process for future revision and comparison (Eyre et al., 2011b). Various surrogates are used to represent the health and condition of the environment being assessed. The BioCondition Assessment Tool uses cameras on mobile devices to take visual evidence of flora and uses an interactive means to identify the flora. Keeping a visual record and associating this with a description can be used by experts at a later stage for validation purposes. Repeated measurements and comparisons of the BioCondition Index provides a measure of how well a terrestrial ecosystem is functioning and this can then be linked to biodiversity values. It should be noted that BioCondition is more geared to be used at the local or property scale.

In Victoria, the Department of Sustainability and Environment has developed the Habitat Hectares method for estimating the quality of an area of vegetation (Parkes et al., 2003). It is mainly geared towards native vegetation and includes site-based measures of quality and quantity of vegetation and condition within the landscape context. Habitat Hectares provides a step-by-step approach to habitat and landscape assessment in the field and includes useful tips for ensuring consistency of application. Vegetation condition is determined by utilizing variables such as presence and amounts of weeds, amounts of log and leaf litter, cover and diversity of understory, and canopy cover and presence of older trees. Repeat measurements and comparisons against pre-determined benchmarks allows for the calculation of native vegetation losses and gains.

BioMetric is a terrestrial biodiversity assessment tool used in New South Wales (Gibbons et al., 2008, 2009). It is mainly applicable for assessment at the paddock or property scale and assesses losses of biodiversity from proposed activities, gains in biodiversity from proposed offsets, or gains in biodiversity as a result of management actions. In BioMetric, the vegetation is assessed against benchmarks, which are quantitative measures of the range of variability in the condition compared to pre-European settlement. Vegetation condition benchmarks are available by vegetation class and BioMetric compares the current or predicted future condition against this benchmark to denote scores that are then converted to a metric.

Currently, no satellite or aircraft data products are used to determine BioCondition, Habitat Hectares, or BioMetric, although research is being conducted in this area. To conclude, monitoring rangeland biodiversity is the basis of management in Australia, so the question is how biodiversity could be measured more efficiently and accurately by remote sensing.

12.2.3 Assessing Rangeland Health by Remote Sensing

Rangeland health is the degree to which soils and vegetation are maintained which would sustain the kinds and amounts of vegetation that would typically occur for that site (NRC, 1994; Pyke et al., 2002). A series of 17 qualitative indicators (with two optional indicators, Table 12.1) are intended to help people with some training to determine rangeland health on the ground in a consistent manner. An overall rating of rangeland health is determined by a preponderance of evidence (Pellant et al., 2005).

Multiple indicators of rangeland health (Table 12.1) are related to the ecological processes leading to transitions between alternative states at an ecological site (Caudle et al., 2013). These indicators may show that a site is either at risk for a transition or has crossed the threshold to an alternative state (Figure 12.1) when monitored on the ground (Herrick et al., 2005a, 2005b). Probably, not all indicators need to be determined (MacKinnon et al., 2011); the three most important in Table 12.1 are:

1. Bare ground cover (Indicator 4),
2. Vegetation composition (Indicator 12), and
3. Presence of invasive species (Indicator 16).

Gaps of bare ground may be the single most-important indicator for rangeland health (Booth and Tueller, 2003).

TABLE 12.1

Indicators of Rangeland Health (Pellant et al., 2005). By examining several qualitative indicators to establish a "preponderance of evidence," an overall assessment of soil and site stability, hydrologic function, and biotic integrity may be made. In the third column, we suggest the potential remote sensing methods suitable for monitoring the indicator.

Rangeland Health Indicator	Assessment	Potential Data Type*
1. Rills in soil	Active soil erosion by water	HSR
2. Water flow patterns	Water infiltration/runoff	HSR
3. Pedestals/terracettes	Active soil erosion by wind or water	
4. Bare ground cover/gap sizes	Potential soil erosion by wind or water	HSR, Hysp, Medium resolution
5. Gullies	Active soil erosion by water	HSR, LiDAR
6. Wind-scoured/deposition areas	Active soil erosion by wind	HSR
7. Litter movement	Soil erosion by wind or water	HSR
8. Soil surface resistance to erosion	Soil quality	
9. Soil surface loss/degradation	Soil quality	
10. Community composition and distribution	Water infiltration/runoff	HSR
11. Compaction layer	Water infiltration/runoff	
12. Vegetation composition/functional groups	Biogeochemical cycles	HSR, Hysp
13. Plant mortality/decadence	Population dynamics	HSR
14. Litter amount	Soil quality	Hysp
15. Net primary production/green leaves	Biogeochemical cycles	fPAR
16. Invasive plants	Population dynamics and biogeochemical cycles	HSR, Hysp, fPAR
17. Perennial plant reproduction	Population dynamics	HSR
18. Biological crusts on soil (optional)	Soil quality	Hysp
19. Vertical vegetation structure (optional)	Animal communities	HSR, LiDAR

* Abbreviations are: HSR—high spatial resolution, Hysp—high spectral resolution (hyperspectral), LiDAR—light detection and ranging, fPAR—high temporal resolution estimating the fraction of absorbed photosynthetically active radiation.

Table 12.1 (third column) lists the potential data sources for 15 of the 19 indicators. The data resolution, which provides the information about an ecological process, is given instead of the sensor name, because the spectral, temporal, and spatial resolutions overlap among different sensors. For detecting gaps of bare ground (Indicator 4), HSR provides direct measurements of cover, whereas hyperspectral (Hysp) and medium resolution data could be used either for direct estimates using spectral unmixing or indirect estimates using spectral indices.

Image classification for vegetation composition (Indicator 12) is one of the primary applications and research areas in remote sensing (Lu and Weng, 2007; Franklin, 2010). In general, the two methods for classification are supervised and unsupervised (Maphanga et al., 2022, Questad et al., 2022, Dube et al., 2021). Supervised classification uses known areas on the ground to create rules (training) for assigning a pixel to a specific category. Unsupervised classification groups similar pixels, which are assigned to different categories afterwards. Independent areas on the ground are then used for assessing the accuracy of the classification (Congalton and Green, 2008; Olofsson et al., 2013). Based on the PROSAIL model (Jacquemoud et al., 2009), the major interacting variables affecting spectral reflectance from a plant canopy are: (1) leaf area index; (2) plant structure and leaf angle distribution; (3) soil background reflectance; (4) positions of the Sun, target, and sensor; and (5) leaf spectral reflectance and transmittance. A plant community or functional type will have similar structural and spectral properties, and to the extent they have constant leaf area index and plant density on similar landscapes, the community or functional type will comprise a single class on an image.

Remote sensing of invasive species (Indicator 16) is based on some detectable difference between the invasives and native species (Ocholla et al., 2024, Thornley et al., 2023, Questad et al., 2022, Hunt et al., 2003; Underwood et al., 2003; Asner, 2004; Madden, 2004; Franklin, 2010; He et al., 2011; Pu, 2012; Bradley, 2013), either spectrally (Section 11.4.2), temporally (Section 11.5.3), or spatially (Section 11.6.3). Most invasive plant species need to be detected at the initial stages of infestation for control, perhaps limiting the usefulness of medium resolution and high temporal resolution sensors. In the Western United States alone, there are more than 300 species of invasive weeds. According to DiTomaso (2000), the five most problematic are:

(1) downy brome (*B. tectorum* also called cheatgrass);
(2) yellow star thistle (*Centaurea solstitialis* L.);
(3) spotted knapweed [*C. stoebe* L., the synonym *C. maculosa* is more common in the literature];
(4) diffuse knapweed (*C. diffusa* Lam.); and
(5) leafy spurge (*Euphorbia esula* L.).

Added to this list is tamerisk (*Tamerix* spp., also called salt cedar), a shrub spreading along rivers and streams in the western United States (Nagler et al., 2011).

12.2.4 Remote Sensing for Animal Biodiversity

The use of remote sensing to estimate animal diversity is increasing. Leyequien et al. (2007) listed five variables that relate to animal needs for food and shelter (Table 12.2). Habitat suitability uses land-cover class determined with medium resolution satellite data, particularly bird species (Gottschalk et al., 2005). Productivity and phenology (Variables 2 and 3, Table 12.2) are important variables that are determined from high temporal resolution data which are related to animal biodiversity (Pettorelli et al., 2011). Correlations between animal species diversity and plant production were established before satellite data were available (Gaston, 2000), although the underlying causes for the correlations are being debated. Habitat structure (Variable 4, Table 12.2) combines several attributes in a given area: variation the amount of bare soil and vegetation, variation in the occurrence of PFTs, and variation of shadows related to the vertical structure of vegetation. Estimates

TABLE 12.2
Variables for the Remote Sensing of Animal Biodiversity According to Leyequien et al. (2007)

Variable	Potential Data Type*
1. Habitat suitability	Medium resolution
2. Photosynthetic productivity	fPAR
3. Multi-temporal patterns	fPAR
4. Habitat structure	Medium resolution, LiDAR, HSR
5. Forage quality	Hysp

* Abbreviations defined in Table 12.1.

of image heterogeneity are strongly related to habitat structure and biodiversity (Section 11.3.2). Vertical habitat structure is measured directly at high spatial resolution using either Light Detection and Ranging (LiDAR) or stereo HSR. Forage quality (Variable 5, Table 12.2) depends on the protein and fiber consumed by herbivores, and may be detectable with hyperspectral remote sensing (Section 11.4.2) or with commercial satellite sensors that have bands at the red-edge of the chlorophyll absorption spectrum.

12.3 MEDIUM RESOLUTION REMOTE SENSING

The Landsat series of satellites are the archetype of medium resolution remote sensing and have provided data globally for over 40 years. Landsat's 4 and 5 carried the Thematic Mapper (TM) sensor (Figure 12.2), Landsat 7 carries the Enhanced Thematic Mapper Plus (ETM+), and the recently launched Landsat 8 carries the Operational Land Imager (OLI) with two new bands (Figure 12.2).

Red and near-infrared spectral indices have been a standard method in analysis of multispectral data since the Landsat 1 was launched to enhance differences between soil and vegetation (Figure 12.2) and to reduce effects of atmospheric transmittance and solar irradiance from either time of year or topography. The spectral indices used most frequently in remote sensing are the Normalized Difference Vegetation Index (NDVI, Rouse et al., 1974; Tucker, 1979), the Soil Adjusted Vegetation Index (SAVI, Huete, 1988), and the Enhanced Vegetation Index (EVI, Huete et al., 2002).

Seasonal and annual precipitation totals in rangelands have high variability, so drought is relatively frequent. Vegetation index differences among images acquired on the same day of the year for different years may be from: (1) drought, (2) recent grazing, (3) fire, or (4) a state change of the ecological site. Long-term monitoring is the only way to distinguish among these possibilities to account for the natural range of variation at a single ecological site (Parracciani et al., 2024; Angerer et al., 2023; Maphanga et al., 2022; Questad et al., 2022; Washington-Allen et al., 2006; Bastin et al., 2014). Comparisons of vegetation indices for a specific area in relation to the average for all areas of that ecological site will highlight areas that have changed or in the process of changing to another ecological state (Maynard et al., 2007; Williamson et al., 2012).

Wildlife and livestock grazing patterns in rangelands are not random; they selectively graze areas with high forage quality (Angerer et al., 2023; Kleinhesselink et al., 2023; Sawalhah et al., 2018; Jafari et al., 2017; McCord et al., 2017; Ramoelo et al., 2012; Zengeya et al., 2013). There are several management changes that affect livestock grazing patterns at the landscape scale, such as fences and locations for water (Kleinhesselink et al., 2023; Questad et al., 2022; Jafari et al., 2017; McCord et al., 2017; Washington-Allen et al., 2004; Bastin et al., 2012). In contrast, wildlife feed in areas with sufficient cover from predators. In the future, determining the non-random grazing patterns at a landscape scale may be important information to manage biodiversity.

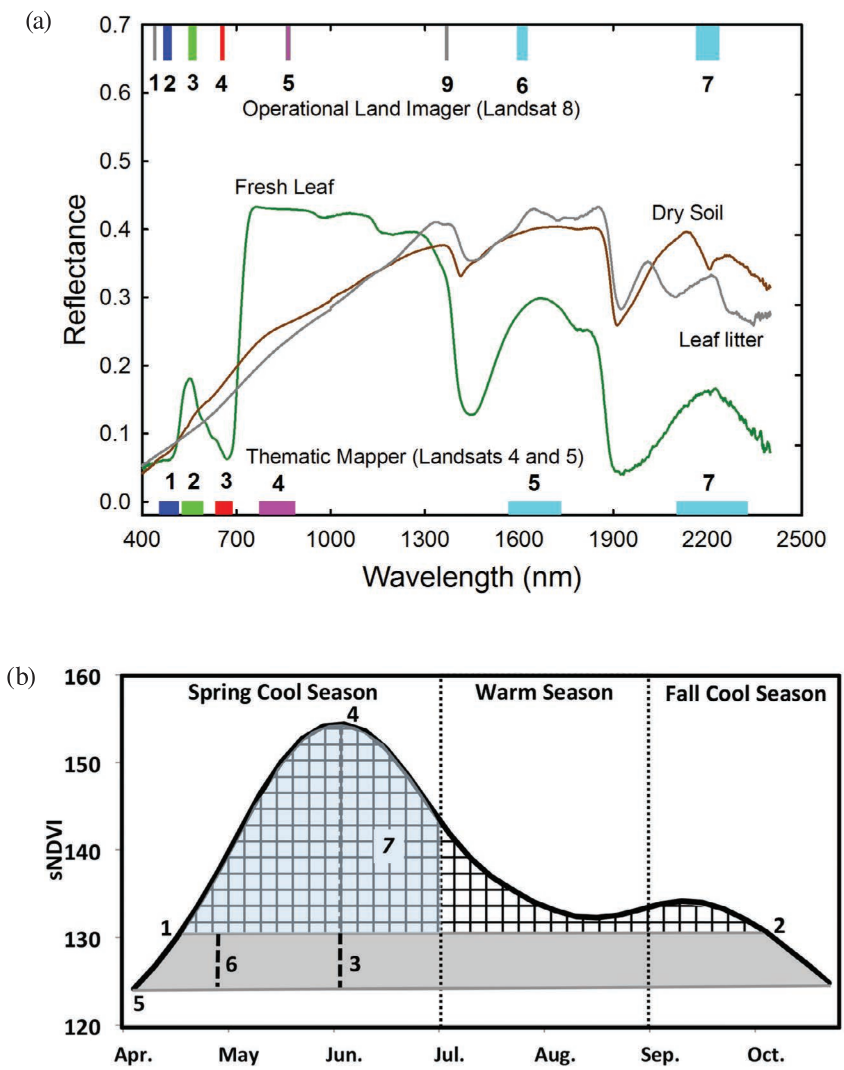

FIGURE 12.2 Spectral reflectances of a healthy green leaf (green line), old leaf litter (gray), and dry soil (brown line). Along the bottom are the wavebands for the Landsats 4 & 5 Thematic Mapper and along the top are the wavebands for the Landsat 8 Operational Line Imager. The width of each bar shows the spectral width of each waveband.

12.3.1 Spectral Unmixing

There is a large spectral difference between vegetation and soils, primarily at red and near-infrared wavelengths (Figure 12.2). Differences in the short-wave infrared region are small if the vegetation and soil are either dry or moist, and are large if the leaves are moist and the soils are dry (Figure 12.2). Linear spectral mixture models are generally thought of as a method for analyzing hyperspectral data (Roberts et al., 1993); however, Adams et al. (1986) developed this method using multispectral data. There are several important assumptions for linear spectral unmixing:

1. The fractional covers are non-negative and sum to one,
2. No multiple scattering among the spectral components (endmembers), and
3. All of the spectral components are known.

Distinct patches of vegetation, litter, and bare soil meet these assumptions; whereas within a patch of vegetation, multiple scattering between individual plants and soil creates nonlinear mixing.

The simplest case of a linear spectral mixture model has two spectral components (S_1 and S_2):

$$S_\lambda = f\,S_1 + (1 - f)\,S_2 \tag{12.1}$$

where S_λ is the sensor measurement, f is the percentage of the first component, and $(1 - f)$ is the percentage of the second component. If the two components are vegetation and soils (Figure 12.2), Equation 12.1 may be rearranged and solved for f:

$$f = (S_\lambda - S_2)/(S_1 - S_2) \tag{12.2}$$

thus, the percentage of bare soil may be calculated directly from the sensor data, and an indicator of rangeland health becomes unambiguously measured.

From Equation 12.2, vegetation indices based on near-infrared (NIR) and red wavebands are nonlinearly related to the fractional cover of vegetation and soil (Jiang et al., 2006; Montandon and Small, 2008). Empirical relationships between fractional cover and vegetation indices have problems because there is a large amount of variability in soil spectra, particularly in rangelands where plant cover is low. Equation 12.2 is also used to normalize NDVI for a site (S_λ) based on maximum NDVI for the year (S_1) and minimum NDVI for the year (S_2), where f is called the vegetation condition index (Kogan et al., 2003).

Equation 12.1 may be extended to include other spectral components such as plant litter, other non-photosynthetic vegetation, and crop residue (Retallack et al., 2023; Maphanga et al., 2022; Sawalhah et al., 2018; Davidson et al., 2008; Guerschman et al., 2009). In some areas, broadband spectral indices may be used to calculate plant litter cover based on statistical regressions (Thornley et al., 2023; Fenetahun et al., 2022; Sawalhah et al., 2018; McNairn and Protz, 1993; van Deventer et al., 1997; Marsett et al., 2006). However, it is often difficult to distinguish bare soil from plant litter with medium-resolution data, particularly when the soil and litter are moist (Daughtry and Hunt, 2008).

12.3.2 Habitat Heterogeneity and Structure

In general, landscapes with a large diversity of cover types and vertical structure also have a high amount of species diversity (Kouba et al., 2024; Kleinhesselink et al., 2023; Maphanga et al., 2022; Questad et al., 2022; Jafari et al., 2017; McCord et al., 2017; Fuhlendorf and Engle, 2001; Tews et al., 2004; Gillespie et al., 2008). Image texture is a general term for the amount of heterogeneity in gray-scale values surrounding a pixel, and there are different statistical formulae (randomness, variance, skewness, entropy, correlation, and more) used for calculating texture (Ocholla et al., 2024; Retallack et al., 2023; Questad et al., 2022; Dube et al., 2021; Haralick et al., 1973; Franklin and Wulder, 2002; Wood et al., 2012). It is recognized that heterogeneity is a function of scale (Haralick et al., 1973; Franklin and Wulder, 2002), so image texture needs to be evaluated with both medium resolution data and higher-resolution commercial satellite data (Johansen and Phinn, 2006).

Plant species richness is strongly related to remotely sensed texture for different regions (Gould, 2000; Dobrowski et al., 2008). Commercial satellite sensors such as DigitalGlobe's WorldView-2 have a panchromatic band with about 0.5-m pixel resolution and multispectral bands with about 2-m pixel resolution. Plant species richness can be determined with these data using various methods of analysis (Parracciani et al., 2024; Thornley et al., 2023; Dube et al., 2021; Hall et al., 2012; Mansour and Mutanga, 2012; Adelabu et al., 2013; Dalmayne et al., 2013; Müllerová et al., 2013). When pixels are smaller than image features, object-based classification creates clusters from adjacent pixels based on spectral information and texture (Yu et al., 2006; Dobrowski et al., 2008; Blaschke, 2010).

Remotely sensed image texture may have more information when flow direction of water and other resource flows are included. Ludgwig et al. (2000, 2002) developed a spatial index (Leakiness) to examine the connections among patches of bare soil, which is related to water flow patterns and the potential to lose soil and nutrients. Later, Ludwig et al. (2006, 2007), using ideas based on spectral unmixing, extended the Leakiness index to landscapes using Landsat Thematic Mapper data.

Habitat suitability for a given bird species is usually known, so land cover data from medium resolution satellites have been used to predict species distribution (Gottshalk et al., 2005). Small scale disturbances create mosaics of different vegetation types and the resulting heterogeneity was associated with greater species richness (Fuhlendorf et al., 2006). Image texture is sensitive to small variations of both vertical structure and vegetation mosaics for determination of bird species richness in a variety of habitats (Retallack et al., 2023; Questad et al., 2022; Sawalhah et al., 2018; Jafari et al., 2017; McCord et al., 2017; St. Louis et al., 2009; Bellis et al., 2008; Culbert et al., 2012; Wood et al., 2013).

12.3.3 Assessment of Medium Resolution

During most of the operational life of Landsats 4 and 5, the data were licensed commercially and thus had limited availability for rangeland management. The economic value per area of rangeland is low, but the total value is high because of the large areas of rangelands on Earth. The U.S. Geological Survey has made the entire archive of Landsat data available free of charge (http://landsat.usgs.gov), and analysis of this long-term archive will provide important insights into the patterns and processes of ecological states (Retallack et al., 2023; Thornley et al., 2023; Fenetahun et al., 2022; Maphanga et al., 2022; Jafari et al., 2017; McCord et al., 2017; Washington-Allen et al., 2006; Hernandez and Ramsey, 2013; Bastin et al., 2014).

We included the new commercial satellites (IKONOS, GeoEye, and WorldView) with pixel sizes between 2 and 5 m for the multispectral bands in this section, because the commercial sensors will be analyzed in large part with the same techniques that are currently used to analyze medium resolution data. Specifically, commercial satellite data will be used to estimate vegetation biomass using spectral vegetation indices, classify habitat suitability from land cover, and estimate vegetation structure with image texture. Some commercial satellite sensors include a band at the red edge of the chlorophyll absorption spectrum, which provides better information on forage quality compared to current medium resolution sensors. But the main disadvantage of commercial satellites is that these are pointed to specific areas, thereby missing adjacent areas on that satellite orbit.

12.4 HIGH SPECTRAL RESOLUTION

Acquisition and analysis of high spectral resolution data, properly called imaging spectrometer data, but ubiquitously called hyperspectral remote sensing, obtains radiance data in numerous, narrow, contiguous bands over a target (Green et al., 1998). With atmospheric correction, the reflectance spectrum of the target is calculated (Gao et al., 1993). From the reflectance spectrum, the identity of the target is determined based on chemical composition.

Linear spectral unmixing may be able to distinguish one spectral component (endmembers) more than the number of bands (Equation 12.1), if the components are known. However, the reflectances at one waveband are highly correlated with those nearby, so the effective number of spectral components is much less than the number of bands (Thorp et al., 2013). Usually, the number of spectral components is not known, or there is multiple, nonlinear scattering among them, which increases the complexity of the spectral unmixing.

Spectral matching compares a pixel's spectrum with some reference spectrum acquired from: a spectral library, field-acquired spectra, or the image itself. The advantage of spectral matching is that the total number of component spectra in the mixture does not need to be known. It must be decided *a priori* the amount of similarity for a match; a typical value for a match is 5.7 °

or 0.1 radians. The common spectral matching algorithms are: the Spectral Angle Mapper (SAM, Kruse et al., 1993), Mixture Tuned Matched Filter (MTMF, Boardman and Kruse, 2011), Spectral Information Divergence (SID, Chang, 2000), Spectral Correlation Measure (SCM, van der Meer, 2006), and Tetracorder (Clark et al., 2003).

SAM calculates a vector angle (Θ) between a reference spectrum $\mathbf{R} = (R_{\lambda 1}, R_{\lambda 2}, \ldots, R_{\lambda n})$ and a target spectrum $\mathbf{T} = (T_{\lambda 1}, T_{\lambda 2}, \ldots, T_{\lambda n})$, where λ1 to λn are the spectral wavelengths:

$$\Theta = \arccos\,[(\mathbf{R} \cdot \mathbf{T})/(\|\mathbf{R}\|\,\|\mathbf{T}\|)] \tag{12.3}$$

where $\|\mathbf{R}\|$ and $\|\mathbf{T}\|$ are vector normalizations and $\mathbf{R} \cdot \mathbf{T}$ is the vector dot product. The spectral angle between the leaf and soil spectra in Figure 12.2 is 28 /° or 0.49 radians. A major advantage (or disadvantage in some instances) of SAM is that differences in brightness are removed by the vector normalization, so large values of Θ are from spectral differences only.

12.4.1 Spectral Separability of Plant Species

The challenge using SAM and other spectral matching algorithms is determining the threshold value for determining a match, so that there are not large numbers of false positives and false negatives. A large threshold value will increase the number of false negatives and a small threshold value will increase the number of false positives. The value also depends on the variability of the target and reference spectra; therefore, how variable are the spectra from different species? To minimize the variation within a species, 10 leaves were acquired from four species growing in a common garden.

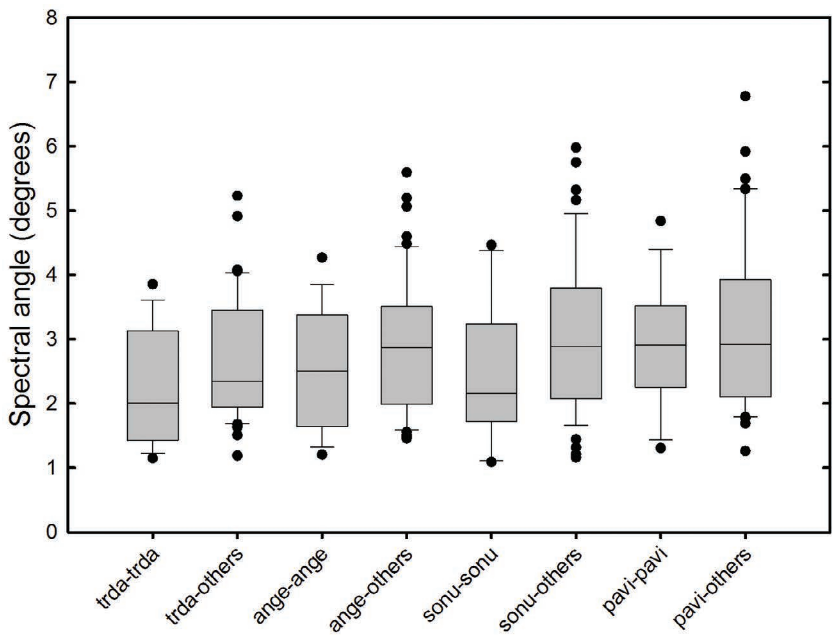

FIGURE 12.3 Spectral angles from leaf spectral reflectances (400–2,400 nm) for four grass species: *Tripsacum dactyloides* (L.) L. (trda, gamagrass); *Andropogon gerardii* Vitman (ange, big bluestem); *Sorghastrum nutans* (L.) Nash (sonu); and *Panicum virgatum* L. (pavi, switch grass). Mean spectra were calculated for each species and used for the reference spectrum, which was compared to the individual leaf spectra of that species (e.g., trda-trda) and spectra from the other species (e.g., trda-others). The center line is the median, the boxes show the range from the 25th to 75th percentiles, the error bars show the range from the 10th and 90th percentiles, and outliers are shown as single points.

Spectral reflectances were measured using a field portable spectrometer collecting light from an integrating sphere (Hunt et al., 2004).

The median spectral angles within a species were less than the median angles compared to the other species (Figure 12.3). The largest separations of spectral angles between within-species and among-species were for *Tripsacum dactyloides* (L.) L. and *Sorghastrum nutans* (L.) Nash. Using the default angle for classification (5.7° or 0.1 radians), only 5 leaves of three species were not spectrally similar to the others.

These results were expected based on previous results (Kouba et al., 2024; Kleinhesselink et al., 2023; Fenetahun et al., 2022; Jafari et al., 2017; McCord et al., 2017; Carter et al., 2005; Clark et al., 2005; Irisarri et al., 2009; Cho et al., 2010; Martin et al., 2011). Furthermore, the PROSPECT leaf optics model (Jacquemoud et al., 1996, 2009; Feret et al., 2008) accurately predicts leaf reflectance and transmittance with only four parameters: the chlorophyll content, the liquid water content, the dry matter content, and a leaf structure parameter equivalent to the number of parallel plates reflecting and transmitting radiation. Therefore, there may not be sufficient degrees of freedom to differentiate species using SAM or other methods (Mansour et al., 2012). Spectral absorption of radiation is based on the types and amounts of chemical bonds (Shenk et al., 2008), so while there may be unique organic compounds in different plant species, there will be few differences in the types and amounts of the chemical bonds. Differences in leaf structure are also highly variable and depend on the conditions during leaf development. Leaf water and chlorophyll contents are affected by current environmental conditions; so much of the variation in leaf reflectance spectra is not related to species.

12.4.2 Plant Chemical Composition

High spectral resolution data have potential for determining forage quality (Variable 5, Table 12.2), which is important for estimating animal biodiversity and livestock distribution (Parracciani et al., 2024; Fenetahun et al., 2022; Jafari et al., 2017; McCord et al., 2017; Leyequien et al., 2007; Skidmore et al., 2010; Knox et al., 2011). Near-infrared (NIR) spectroscopy is a standard laboratory method for analysis of dried plant materials for protein and fiber contents (Shenk et al., 2008), and hyperspectral sensors provide coverage of the same wavelength regions. One problem is determination of forage quality when the vegetation has high water content, because the spectral absorption of water dominates the SWIR reflectance spectrum (Ramoelo et al., 2011; Ustin et al., 2012). As the spectral absorption coefficients for liquid water are reasonably well known (Ustin et al., 2012), it is possible to remove the spectral features caused by water to estimate proteins and dry matter (Ramoelo et al., 2011; Wang et al., 2011b). Extensive studies with field spectrometers show strong potential for determination of forage quality (Starks et al., 2004; Knox et al., 2011), but the algorithms require extensive calibration and may not be appropriate for other species at other locations.

The areal cover of bare soil and litter are important indicators of rangeland health (Indicators 4 and 14, respectively, Table 12.1) and are readily detectable using high spectral resolution data (Figure 12.1). Cellulose and lignin are synthesized by plants and these substances are not found in soil, so narrow-band indices emphasizing spectral features in the shortwave infrared (SWIR) are linearly related to the cover of litter over bare soil (Ocholla et al., 2024; Kleinhesselink et al., 2023; Maphanga et al., 2022; Jafari et al., 2017; McCord et al., 2017; Daughtry, 2001; Nagler et al., 2003; Serbin et al., 2009, 2013). SWIR absorption features of bare soil (Figure 12.1) exposed from erosion are also detectable the Advanced Spaceborne Thermal Emission and Reflection Radiometer (ASTER) on NASA's Terra satellite (Maphanga et al., 2022; Questad et al., 2022; Dube et al., 2021; Matongera et al., 2021; Vrieling et al., 2007; Gill and Phinn, 2008; Serbin et al., 2009).

Biological soil crusts (Indicator 18, Table 12.1) are mixtures of cyanobacteria, fungi, and bacteria that form on the soil surface in arid and semiarid ecosystems. Chlorophyll a in the cyanobacteria creates a small absorption feature at 680 nm wavelength distinct from soil (Karnieli et al., 2003; Weber et al., 2008; Ustin et al., 2009). The problem is that the chlorophyll-a feature is also found in algae, lichens, moss, and plants; reflectances in the SWIR allow separation of biological soil crusts from small amounts of plants and plant-like classes (Ustin et al., 2009).

12.4.3 Detection of Invasive Plant Species

Whereas leaves of most rangeland species may not have much spectral diversity, distinctive leaves and flowers of invasive plants may result in characteristic spectral signatures that may be detected with high spectral resolution data (Table 12.3). Leafy spurge is a noxious invasive weed infesting large areas of the U.S. Great Plains. It is clonal, forming dense stands of genetically identical aboveground shoots spreading from a single root system. Flowers are clustered at or near the top of the shoot (umbels) and the flower cover is frequently over 20% in a single clone (Hunt et al., 2007). The flower bracts' yellow-green color is from a small amount of chlorophyll and a large ratio of carotenoids to chlorophylls (Hunt et al., 2004). When leafy spurge is found, one management option is the release of insects that specifically feed on the roots (larvae) and shoots (adult) for biological control (Thornley et al., 2023; Questad et al., 2022; Dube et al., 2021; Jafari et al., 2017; Anderson et al., 2003; Lym, 2005; Samuel et al., 2008; Lesica and Hanna, 2009).

Hyperspectral sensors are successful in detecting leafy spurge based on the yellow-green bracts (Retallack et al., 2023; Dube et al., 2021; Jafari et al., 2017; McCord et al., 2017; O'Neill et al., 2000; Parker Williams and Hunt, 2002, 2004; Dudek et al., 2004; Glenn et al., 2005; Lawrence et al., 2006). Furthermore, medium-resolution satellite sensors generally were not very successful (Retallack et al., 2023; Maphanga et al., 2022; Matongera et al., 2021; Sawalhah et al., 2018; McCord et al., 2017; Hunt and Parker Williams, 2006; Mladinich et al., 2006; Stitt et al., 2006; Hunt et al., 2007). The flower bracts of leafy spurge are readily detectable with aerial photography and videography (Anderson et al., 1996).

Parker Williams and Hunt (2002, 2004) analyzed two Airborne Visible Infrared Imaging Spectrometer (AVIRIS) scenes acquired on July 6, 1999 over Devils Tower National Monument and surrounding areas in Crook County, Wyoming. Two sets of plots were acquired, one with the cover of leafy spurge estimated ($N = 66$) and one with a simple classification of presence or absence ($N = 146$). Two scenes were atmospherically corrected to land-surface reflectance using the ATREM version 3.1 program (Gao et al., 1993) and processed using the "Spectral Hourglass" approach (Boardman and Kruse, 2011). Dimensionality was reduced using the Minimum Noise Fraction (MNF) in the Environment for Visualizing Images (ENVI version 3.2, Research Systems Inc.), and spectral signatures for leafy spurge were picked from the AVIRIS images using the Pixel Purity Index and n-Dimensional Visualizer (Boardman and Kruse, 2011).

The Mixture Tuned Matched Filter (MTMF, Boardman and Kruse, 2011) was used to identify pixels with possible leafy spurge. The MTMF score was related to leafy spurge cover with an R^2 of 0.66 (Parker Williams and Hunt, 2002), and the classification accuracy was 87% (Parker Williams and Hunt, 2004). However, accuracies of leafy spurge detection with MTMF appear to be dependent on the number of other spectral signatures in a scene (Fenetahun et al., 2022; Maphanga et al., 2022; Questad et al., 2022; Dudek et al., 2004; Glenn et al., 2005; Mitchell and Glenn, 2009). Using the data from Parker Williams and Hunt (2002, 2004), 11 AVIRIS scenes were combined into a single image for analysis; the overall classification accuracy using MTMF was no better than chance (Hunt et al., 2007). The type of spectral mixing needs to be considered, differences in plant density may change the amount of nonlinear mixing (Mitchell and Glenn, 2009).

There were many studies using high spectral resolution data to detect invasive species; two species commonly studied were tamarisk and yellow star thistle (Table 12.3). Detection of these invasive species may seem at odds with Figure 12.3 and related studies. In Table 12.3, the reflectance spectra of invasive species were in context with native species, soils, and subtle variations in spatial arrangement, leaf area index or leaf angle distribution. The leaf spectra in Figure 12.3 were isolated from any context. Successful use of hyperspectral data for detection of invasive species were based on knowing the invasive was present and having areas for training of supervised classification algorithms (Underwood et al., 2007).

TABLE 12.3
Invasive Plant Species in Rangelands Identified with High Spectral Resolution Data

Study	Species	Methods*
O'Neill et al., 2000; Parker Williams and Hunt, 2002, 2004; Dudek et al., 2004; Glenn et al., 2005; Hunt et al., 2007; Lawrence et al., 2006; Mitchell and Glenn, 2009	Leafy spurge (*Euphorbia esula* L.)	MNF, MTMF, SAM, supervised classification
Lass et al., 2002	Spotted knapweed (*Centaurea stoebe* L., *C. maculosa* is a commonly used synonym)	SAM
Underwood et al., 2003, 2007	Ice plant [*Carpobrotus edulis* (L. N. E. Br.)], Jubata grass/Pampas grass [*Cortaderia jubata* (Lemoine ex Carrière) Stapf], Blue gum (*Eucalyptus globules* Labill.)	MNF, continuum removal, spectral indices, supervised classification
Anderson et al., 2005	Tamarisk (*Tamarix chinensis Lour.*; T. gallica L.; and *T. ramosissima* Ledeb.)	PC, spectral indices
Lass et al., 2005	Yellow starthistle (*C. solstitialis* L.) and Babysbreath (*Gypsophila paniculata* L.)	SAM
Mundt et al., 2005	Hoary cress (*Cardaria draba* L.)	MNF, MTMF, SAM
Andrew and Ustin, 2006, 2008	Perennial pepperweed (*Lepidium latifolium* L.)	MNF, MTMF
Ge et al., 2006, 2007	Yellow star thistle	Spectral indices, SAM
Miao et al., 2006, 2007	Yellow star thistle	Band selection, feature extraction
Mirik et al., 2006, 2013	Musk thistle (*Carduus nutans* L.)	Regression, SVM
Narumalani et al., 2006, 2009	Tamerisk, Musk thistle, Canada thistle (*Cirsium arvense* L.), Reed canary grass (*Phalaris arundinacea* L.), Russian olive (*Elaeagnus augustifolia* L.)	ISODATA, MNF, SAM
Cheng et al., 2007	Kudzu [*Pueraria montana* (Lour.) Merr.]	MNF, MTMF, SAM
Hamada et al., 2007	Tamarisk	MNF, spectral indices, MTMF, stepwise discriminant analysis, hierarchical clustering, root sum squared differential area
Hestir et al., 2008	Perennial pepperweed, Water hyacinth [*Eichhornia crassipes* (Mart.) Solms], Brazilian waterweed (*Egeria densa* Planch.)	MNF, band indices, spectral mixture analysis, SAM, continuum removal
Noujdina and Ustin, 2008	Downy brome (*Bromus tectorum* L.)	MNF, MTMF
Pu, 2008; Pu et al., 2008	Tamarisk	PC, spectral indices
Wang et al., 2008	Sericea lespedeza [*Lespedeza cuneata* (Dum. Cours.) G. Don]	ISODATA, spectral derivatives
Carter et al., 2009	Tamarisk	MNF, supervised classification
Yang et al., 2009; Yang and Everitt, 2010a, 2010b	Ashe juniper (Juniperus ashei J. Buchholz), Broom snakeweed [*Gutierrezia sarothrae* (Pursh.) Britt. and Rusby], water hyacinth	MNF, SAM, supervised classification
Wang et al., 2010a; Bentivegna et al., 2012	Cut-leaved teasel (*Dipsacus laciniatus* L.)	SAM, supervised classification, spectral information divergence

(Continued)

TABLE 12.3 (*Continued*)
Invasive Plant Species in Rangelands Identified with High Spectral Resolution Data

Study	Species	Methods*
Fletcher et al., 2011; Yang et al., 2013	Tamarisk	SVM
Miao et al., 2011	Tamarisk	MNF, PC, supervised classification, SAM
Olsson and Morisette, 2014	Buffelgrass [*Pennisetum ciliare* (L.) Link]	MNF, MTMF, random forest

* Abbreviations are: minimum noise fraction (MNF), mixture tuned matched filtering (MTMF), spectral angle mapper (SAM), Iterative Self Organizing Data Analysis Technique Algorithm (ISODATA), principal components (PC), and Support Vector Machine (SVM)

12.4.4 Assessment of High Spectral Resolution

There are only two indicators of rangeland health (Table 12.1) and one variable for animal biodiversity (Table 12.2) for which the preferred method of remote sensing is high spectral resolution. The large spectral difference between vegetation and soils allows accurate assessments of relative cover, so one of the three most important indicators is reliably determined with hyperspectral sensors. Compared to other methods, the suitability of hyperspectral remote sensing for rangeland monitoring depends on detection of the other two critical indicators, invasive species and composition of plant functional types. The extensive discussion in Section 11.4.3 shows that more research is required, perhaps using simulated Hyperspectral Infrared Imager (HyspIRI) mission data produced with high-altitude AVIRIS imagery (http://hyspiri.jpl.nasa.gov; last checked June 12, 2014).

Compared to other sensors, it is more expensive to acquire an airborne hyperspectral sensor, and it takes more time and expertise to analyze hyperspectral imagery, so mapping the distribution of an invasive species over a landscape may not be cost effective. Geospatial species-distribution models classify suitable habitat over larger areas based on combinations of climate, vegetation, soils, topography and other variables within a geographic information system. There are too many combinations of factors to establish field plots for complete model testing. Classified hyperspectral imagery for small areas should be used to test species geospatial niche models, and then the geospatial models should be used to classify suitable habitat over larger areas (Kleinhesselink et al., 2023; Questad et al., 2022; Dube et al., 2021; Matongera et al., 2021; Sawalhah et al., 2018; Jafari et al., 2017; McCord et al., 2017; Underwood et al., 2004; Andrew and Ustin, 2009; Hunt et al., 2010).

Global biodiversity is one of the important science questions for the NASA HyspIRI mission (Roberts et al., 2012). The total number of species in a small area (alpha diversity) and the total number of species in a large area (gamma diversity) are more encompassing assessments of biodiversity. Alpha and gamma diversities are inter-related by beta diversity, which is a measure of the proportion of shared species between two points along an environmental gradient. Rocchini et al. (2010a, 2010b) hypothesized spectral diversity is an important method for estimating beta diversity. If this hypothesis is validated, then high spectral resolution data will become invaluable for estimating biodiversity, even though invasive species or plant functional types may not be detected.

12.5 HIGH TEMPORAL RESOLUTION

Repeated satellite acquisitions reveal seasonal patterns and growth of vegetation; however, cloud cover may obscure vegetation during critical time periods of active plant growth. High temporal resolution data acquire data every few days, which are composited to form weekly to monthly cloud-free time series. Even in rangelands, "where the skies are not cloudy all day" (Higley and Kelly, 1873), medium resolution imagery are frequently unusable because of cloud occurrence during the onset of the plant growing season. Meteorological satellites, such as NOAA's Advanced Very High Resolution Radiometer (AVHRR) and NASA's Moderate Resolution Imaging Spectroradiometer (MODIS), use the change in NDVI over the year to determine phenology and the fraction of absorbed photosynthetically active radiation (fPAR). Gross and net primary production are calculated from the total absorbed photosynthetically active radiation and light use efficiency (Hunt et al., 2003). Productivity is an indicator of rangeland health (Indicator 15, Table 12.1) and a variable for predicting animal biodiversity (Variable 2, Table 12.2).

Over a small region, interannual variation in phenology is related to climatic variability (Reed et al., 1994; Schwartz et al., 2002), whereas consistent spatial variation in phenology is related to plant functional type (Kouba et al., 2024; Retallack et al., 2023; Dube et al., 2021; Loveland et al., 1991; Kremer and Running, 1993; Peters et al., 1997; Gu et al., 2010). Grasses (Poaceae) have two functional types based on photosynthetic pathway: cool-season grasses with C_3 photosynthesis, and warm-season grasses with C_4 photosynthesis. Physiologically, C_3 photosynthesis is greater at cool temperatures and C_4 photosynthesis is higher at warm temperatures, but temperature affects many different processes, not just photosynthesis (Sage and Kubien, 2007). With global climatic change, warmer temperature may favor C_4 grasses whereas elevated atmospheric CO_2 may promote C_3 plants (Morgan et al., 2007). Therefore, C_3/C_4 relative abundance is a complex response of climate change, and will affect ecosystem biogeochemical cycles at regional and global scales.

Temperate grasslands in North America, South America, Australia, Africa, and Asia have mixtures of C_3 and C_4 grasses with the ratio depending on the amount of rainfall during the warm and cool seasons (Winslow et al., 2003). Determining the ratios of C_3 and C_4 grasses is a challenge because the reflectance spectra may not be separable (Adjorlolo et al., 2012a, 2012b). High temporal resolution AVHRR or Medium Resolution Imaging Spectrometer (MERIS) data was used to separate C_3 and C_4 grasses (Ocholla et al., 2024; Thornley et al., 2023; Questad et al., 2022; Jafari et al., 2017; McCord et al., 2017; Goodin and Henebry, 1997; Tieszen et al., 1997; Ricotta et al., 2003; Foody and Dash, 2007, 2010). Medium resolution imagery acquired two or three times per year also showed differences based on temperature (Davidson and Csillag, 2001; Peterson et al., 2002; Guo et al., 2003). High temporal resolution data may add more information by subdividing both C_3 and C_4 functional types into tall and short functional types (Wang et al., 2013).

12.5.1 Phenology Metrics

The first step for determining phenological metrics from high temporal resolution data is applying a low-pass filter to the time series of NDVI to remove the effects of sub-pixel clouds, atmospheric conditions, and view angles. Several smoothing algorithms have been used: a nonlinear median filter (Reed et al., 1994), an upper-envelope three-point filter (Gu et al., 2006), and a 2nd-order polynomial filter (Savitzky and Golay, 1964).

Most studies define a series of metrics from the smoothed NDVI time series (Table 12.4). These metrics may be determined by a sequence of logical statements; tools have been developed to automate calculation of the various metrics: fitting the NDVI time series into piecewise logistic functions (Zhang et al., 2003), fitting the time series using a quadratic function (de Beurs and Henebry, 2004), and in the open-source TIMESAT program (Jönsson and Eklundh, 2004). In rangelands, these mathematical approaches may produce errors because grasses often have prolonged growing season and asymmetric trajectories (de Beurs and Henebry, 2010). For this reason, some studies directly use the polynomial-smoothed time series to extract phenological metrics directly (Parracciani et al., 2024; Thornley et al., 2023; Questad et al., 2022; Dube et al., 2021; Matongera et al., 2021; McCord et al., 2017; Wang et al., 2010b, 2011a, 2013).

TABLE 12.4

Common Phenology Metrics for Determining Plant Functional Types. These metrics have to be determined with a complete time series of NDVI.

Metric	Definition
Start of season (*SOS*)	Before Peak NDVI, DOY* when NDVI > threshold
End of season (*EOS*)	After peak NDVI, DOY when NDVI < threshold
Length of season (*LOS*)	*EOS* – *SOS*
Peak NDVI	Maximum NDVI in time series
Peak date	DOY of Peak NDVI
Cumulative NDVI (*Σ-NDVI*)	Sum NDVI when *SOS* < NDVI < *EOS*

* Day of the Year (DOY)

12.5.2 Grass Functional Types

Dividing the U.S. Great Plains at 100° West Longitude, east of this meridian is primarily sub-humid tallgrass prairie with 500–750 mm of annual precipitation (Figure 12.4a). West of this meridian are the southern shortgrass steppe and the northern mixed-grass prairie (Figure 12.4a), which get about 250–500 mm of precipitation annually. Precipitation strongly controls grassland productivity resulting in the designations, tallgrass and shortgrass. The latitudinal C_3/C_4 variations and longitudinal tall/short differences are combined into tallgrass C_3, tallgrass C_4, shortgrass C_3 and shortgrass C_4. The latter three PFTs correspond to naturally occurring ecological regions; however, tallgrass C_3 may be the result of seeding cool-season species (e.g., tall fescue) into pastures for higher forage production (Fenetahun et al., 2022; Sawalhah et al., 2018; Jafari et al., 2017; McCord et al., 2017; Wang et al., 2013).

Grassland areas were determined from the USGS National Land-Cover Database (Homer et al., 2004); the grassland areas were not divided into functional types. Time series of the 500-m, eight-day Terra MODIS Surface Reflectance products (MOD09A1) for the years 2000 to 2009 show phenological variations of C_3 and C_4 grasses (Figure 12.5). Tallgrass C_3 and C_4 have higher NDVI values than shortgrass C_3 and C_4. Summer dormancy and fall growth for tallgrass C_3 was seen in some years as a second NDVI peak in the autumn (Figure 12.5), but this phenological feature was much less important than an earlier start of growing season (*SOS*), later end of growing season (*EOS*), and therefore longer length of growing season (*LOS*). Shortgrass C_3 have much earlier *SOS* than shortgrass C_4 and both have shorter *LOS* than the tallgrass PFTs (Figure 12.5).

The four grass PFTs in the U.S. Great Plains were mapped over the ten-year period (2000–2009) with a decision tree approach (Figure 12.4b). Because of interannual variability in temperature and precipitation, a given pixel would be classified as one PFT for some years and would be classified as another PFT for other years. For example, during drought, tallgrass C_3 and shortgrass C_3 *SOS* may be delayed and *EOS* may be earlier, so that the phenological features become similar to those of tallgrass C_4 and shortgrass C_4, respectively.

Therefore, delineation of grass C_3/C_4 PFTs is problematic using data from only a single year. A long time series of data were required for reliable separation (Winslow and Hunt, 2003; Wang et al., 2013). The final classification in Figure 12.4b displays the distributions where one PFT was selected for at least 6 of the 10 years (Wang et al., 2013). The four PFTs followed the longitudinal transition of ecological regions based on precipitation. However, latitudinal trends caused by temperature were not present, because east of 100 ° West, tallgrass C_3 areas were south of tallgrass C_4 areas. Splitting grasses into tallgrass and shortgrass highlighted the occurrence of a new ecological

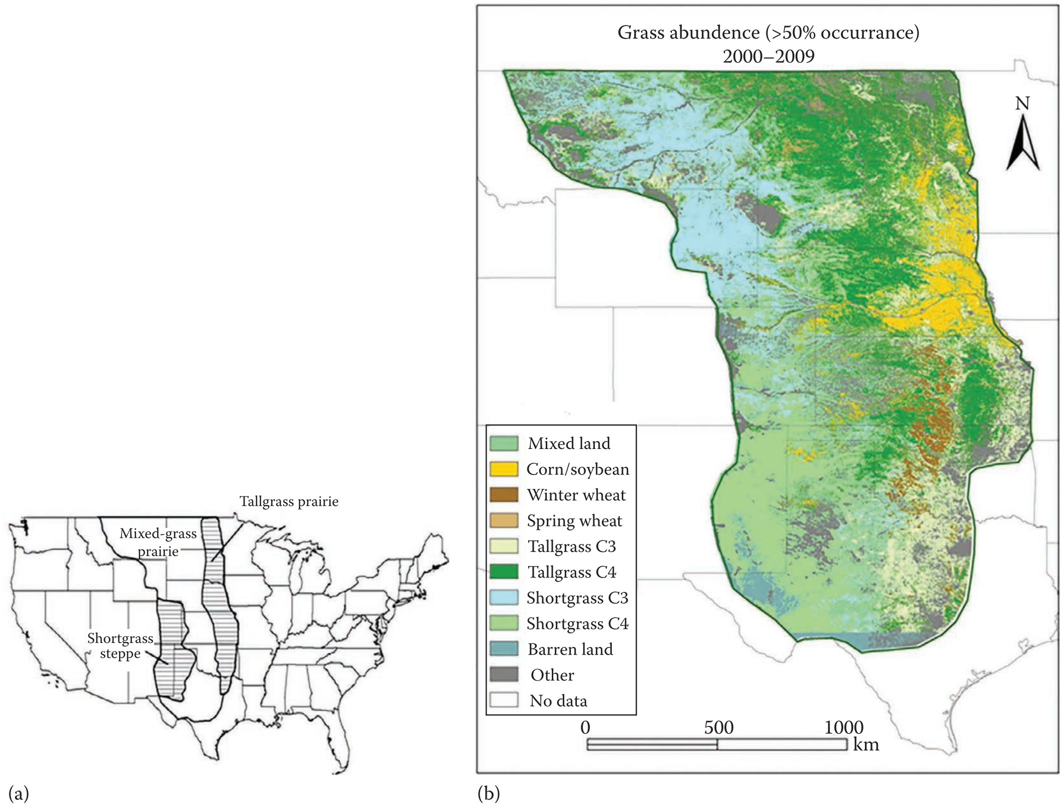

FIGURE 12.4 (a) Ecological regions of the tallgrass prairie, shortgrass steppe, and northern mixed-grass prairie. (b) Distributions of four grass functional types in the U.S. Great Plains: tallgrass C_3, tallgrass C_4, shortgrass C_3, and shortgrass C_3. Tallgrass C_3 is not a naturally occurring ecological region in the U.S. Great Plains and may be the result of seeding C_3 species into pastures. Interannual variability in precipitation and temperature affected phenology, so a functional type had to be selected at least six years from 2000–2009 to be classified that functional type.

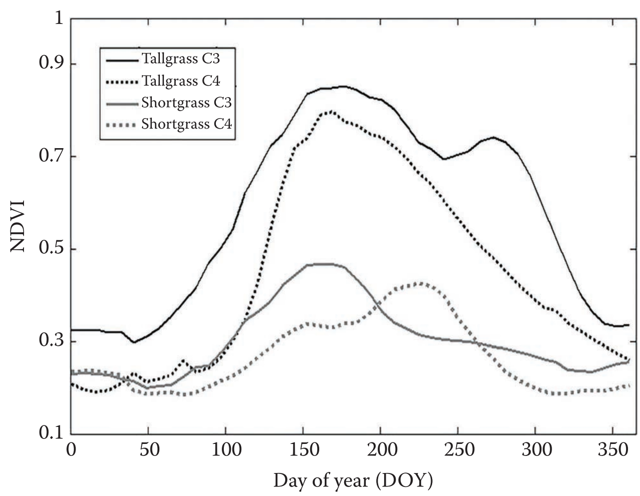

FIGURE 12.5 Examples of NDVI time series of the four grass functional types: tallgrass C_3, tallgrass C_4, shortgrass C_3, and shortgrass C_3. The NDVI values of pure pixels are extracted from the 46 MODIS scenes acquired in 2007.

region; the areas classified as tallgrass C_3 are located in areas generally considered to be pastures (Maphanga et al., 2022; Dube et al., 2021; McCord et al., 2017; Wang et al., 2013). Because more of the variation in temporal profiles was now explained, the resulting classification had somewhat increased accuracy.

12.5.3 Invasive Plant Species

Few invasive species are detected from the large pixels of high temporal resolution data (e.g., AVHRR and MODIS). One species is downy brome in the western United States, Bradley and Mustard (2005, 2006) showed that the temporal variation between downy brome and co-occurring species was large enough to classify downy brome invasion using AVHRR. Singh and Glenn (2009) and Clinton et al. (2010) replicated this study using a time-series of Landsat and MODIS data, respectively.

Two other species that may be detected using high temporal resolution data are broom snakeweed [*Gutierrezia sarothrae* (Pursh) Britton & Rusby; Peters et al., 1992] and Lehmann lovegrass (*Eragrostis lehmanniana* Nees; Huang and Geiger, 2008; Huang et al., 2009). Broom snakeweed is a C_3 shrub surrounded by C_4 grasses, so it was detected based on its earlier *SOS*. Lehmann lovegrass is a C_4 grass that crowds out native C_4 grasses; during senescence it produces a litter layer that is dense, bright and yellow which is detectable even with large pixel sizes (Huang and Geiger, 2008; Huang et al., 2009).

Two important questions about invasive species are addressed using ecological niche or habitat suitability models: (1) what areas on Earth may be susceptible to an invasive species, and (2) how will the areas expand or contract with anthropogenic global warming (Angerer et al., 2023; Fenetahun et al., 2022; Sawalhah et al., 2018; Jafari et al., 2017; Peterson, 2003; Thuiller et al., 2005; Andrew and Ustin, 2009; Stohlgren et al., 2010). MODIS vegetation index data are important for predicting the potential distribution of tamarisk (Morisette et al., 2006) and purple loosestrife (*Lythrum salicaria* L.; Anderson et al., 2006). In these studies, time series of NDVI are used as a surrogate for meteorological data, because even with 1-km pixel size, the data are much more densely distributed compared to available weather station data.

12.5.4 Assessment of High Temporal Resolution

The specifications for NASA MODIS and the recently launched Suomi National Polar-orbiting Partnership Visible Infrared Imaging Radiometer Suite (VIIRS) were developed in part based on the long history of AVHRR for global remote sensing of interannual climatic variability. Most land-cover classifications using AVHRR data were designed to be used by global ecosystem models, so fewer PFTs were defined. Because of limited computing power, there were limitations placed on the spatial resolution in order to provide high-quality data at high temporal resolution (Townshend and Justice, 1988). Therefore, variations in phenology related to taxonomy, plant functional types, and other considerations at smaller scales were rarely explored because of the large pixel sizes.

Two satellite systems have broad swaths and high temporal resolution with much smaller pixel sizes: (1) the Indian Space Research Organization's Advanced Wide Field Sensor (AWiFS) and (2) the international Disaster Monitoring Constellation (Wang et al., 2010c). However, data from these two sensors are only available from commercial venders and are not freely available from public archives (Goward et al., 2012).

With more powerful computers available, tradeoffs between high temporal resolution and high spatial resolution are no longer required. For example, the United States Department of Agriculture (USDA) National Agricultural Statistics Service (NASS) previously used AWiFS data (56–70 m pixels) and currently uses Deimos-1 data (22 m pixels) to produce annual Cropland Data Layers for the USA (Boryan et al., 2011). The potential of high temporal resolution data for monitoring rangeland biodiversity is simply not known. Making AWiFS, Deimos, and similar multispectral sensor data available worldwide is an important investment for monitoring global biodiversity (Retallack et al., 2023; Questad et al., 2022; Dube et al., 2021; Wang et al., 2010c).

12.6 HIGH SPATIAL RESOLUTION

While ground and aerial photographs have been used for natural resource management since the last century (Cooper, 1924), advances in digital sensors and computer processing have made high spatial resolution (HSR) the newest dimension in remote sensing. The term "high spatial resolution" is subjective, changes with time, and can mean pixel sizes from 0.25 mm to 2 m with the current state of the art. Smaller pixel sizes must be acquired from aircraft flying at lower altitudes, usually resulting in smaller areas covered per image (< 1 ha compared to 27,000 ha for WorldView-2 data). HSR images are also referred to as "very-large scale" in reference to the map scale (e.g., 1:500 compared to 1:24,000 for a 7.5 ft × 7.5 ft topographic map).

HSR imagery are useful in most aspects of rangeland resource management including assessments of ground cover, riparian condition, wildlife habitat, woodlands and other resource concerns. One of the characteristics of HSR images is very high pixel to pixel variability, but each pixel is spectrally pure (Figure 12.6). With larger pixel sizes, each pixel is a heterogeneous mixture of different spectral components (Figure 12.6). At the scale of 1 m, spectral unmixing or spectral indices are required to measure the amount of bare ground, so the advantages of HSR satellite data compared to medium resolution satellite data are not clear. On the other hand, at the scale of 0.4-mm HSR aircraft data, the established techniques of remote sensing are inadequate and new techniques

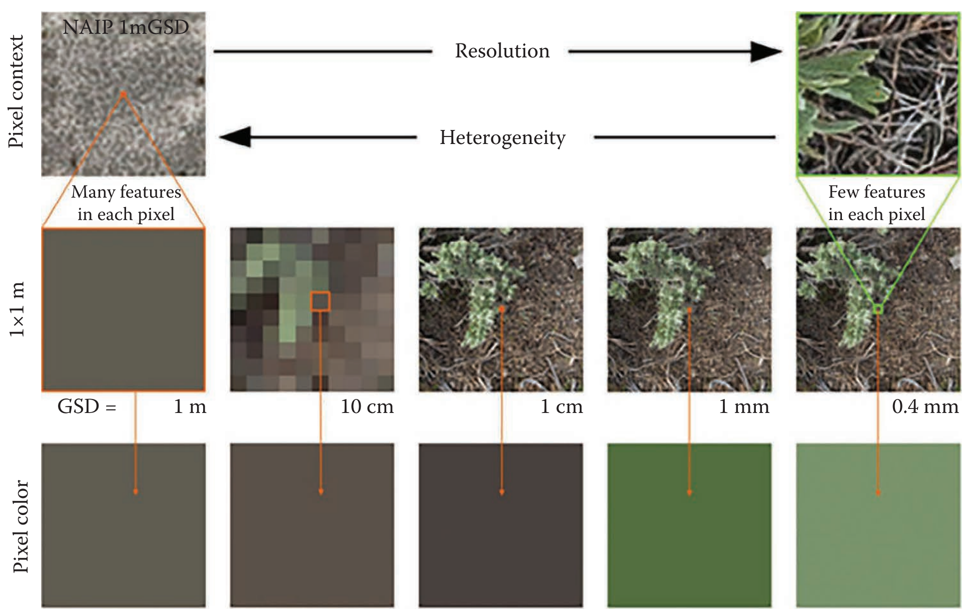

FIGURE 12.6 Effect of spatial resolution (also called ground sample distance) on pixel color and visual interpretation. The top left panel shows a 100 × 100-m area of rangeland in southeast Idaho at 1-m resolution to illustrate the heterogeneity of the imaged area. The middle row shows a 1 × 1-m patch of rangeland in all panels with the lowest spatial resolution on the left (1-m pixel size) and highest resolution on the right (0.4-mm pixel size). The top right panel shows an enlargement of the 0.4-mm resolution image; the red dot in the center (shown by the blue arrow) is one 0.4-mm pixel situated on a sagebrush leaf. The lower row shows pixel color change from increasing resolution from 1 m to 0.4 mm. (Figure adapted from Weber et al. (2013), and used with permission.)

are being developed and tested. Alternatively, established techniques of visual photo-interpretation can often be updated for use with digital imagery. As shown by Figure 12.6, the resolution of HSR data needs to be from 0.25 mm to 10 mm in order to visually interpret the data effectively.

12.6.1 Ground Imaging

Most ground assessments continue to be interpretations and judgments based on monitoring a limited number of non-randomly selected sites. It simply has not been practical to do otherwise. However, ground and aerial digital photography are replacing or augmenting time-consuming field methods, and are increasing the objectivity of rangeland monitoring (Booth et al., 2008; Moffet, 2009; Sadler et al., 2010; Booth and Cox, 2011). Digital photography and subsequent photo interpretation can increase sampling rates over traditional field sampling methods (Kouba et al., 2024; Retallack et al., 2023; Questad et al., 2022; Jafari et al., 2017; McCord et al., 2017 Luscier, 2006; Cagney et al., 2011). Reduced monitoring time and associated labor costs can increase monitoring precision by allowing for increased sample numbers.

Methods for obtaining non-aerial, nadir-looking digital images include a free-hand method (Cagney et al., 2011) and the use of staffs, tripods, stands (Booth et al., 2004; Booth and Cox, 2011), booms, and gantries (Louhaichi et al., 2010), vehicle mounts and other aids to reduce camera motion. Furthermore, these tools allow for a range of camera positions above ground level and a range of image resolutions. For a permanent record, the digital images are archived at much lower cost compared to film negatives or prints. Even where sampling will be done primarily from aircraft, acquisition of ground images is an important part of monitoring since it provides the opportunity to capture nadir images with less motion blur than can be obtained from the air.

12.6.2 Aerial Imaging

Some image users require boundary-to-boundary coverage, and HSR mosaics may be made from airborne data at considerable expense. However, many users do not require mosaics, and can manage effectively at lower cost by capturing single-image samples that are systematically distributed across watersheds, allotments, and other landscape-scale management units (Figure 12.7). Geographic Information Systems (GIS) should be used to draft sampling plans that define intended locations for ground or aerial image acquisition to acquire a statistically adequate sample that represents the natural range of variation in the areas monitored (Blumenthal et al., 2007; Booth and Cox, 2008).

Platforms used for HSR aerial-image acquisition include manned conventional and light sport airplanes (LSAs), manned and unmanned helicopters, and unmanned fixed-wing aircraft (Booth and Cox, 2011). Surprisingly, contracting for a piloted LSA was the least expensive, because fewer personnel were required to be on site for safety. Furthermore, only LSAs and helicopters were able to fly slow enough to avoid excessive motion blur with image resolutions of 1-mm resolution or less (Figure 12.8). Contract costs for manned helicopters are usually more expensive than for LSAs, but helicopters (manned or unmanned) can fly during windy conditions when LSAs cannot safely operate. To mitigate risk, LSAs need to be equipped with rocket-deployed, whole-plane parachutes in the event of mechanical failure. Frequently in windy areas, flights are made early in the day before strong winds and atmospheric turbulence develops. A potential problem with early morning flights is presence of shadows that may affect estimates of bare ground cover.

Manned helicopters and LSAs can carry multiple cameras allowing for nested, simultaneously acquired, multi-resolution images; for example: 1-, 10-, and 20-mm pixel sizes. This capability allowed users to acquire wide fields of view *and* high resolution, a capability that proved important for the study of fire intervals in shrub ecosystems (Moffet, 2009), and monitoring invasive species (Kouba et al., 2024; Retallack et al., 2023; Maphanga et al., 2022; Questad et al., 2022; Dube et al., 2021; Blumenthal et al., 2007, 2012; Booth et al., 2010).

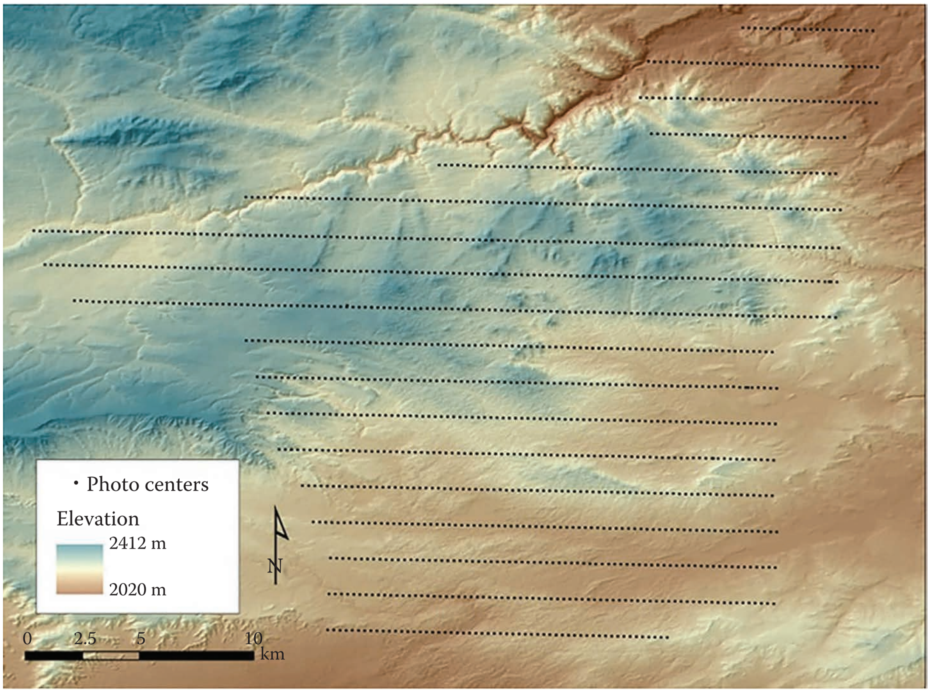

FIGURE 12.7 Flight plan in Wyoming's Red Desert (center: 43.37°N, 108.40°W) showing 1,457 image acquisition points which were 200 m apart along east-west flight lines spaced 1600 m apart. Three images were collected at each acquisition point: (1) an area of 3 × 4 m with 0.9-mm pixels; (2) an area of 24 × 36 m, with7-mm pixels; and (3) an area of 48 × 72 m with 14-mm pixels.

Aerial surveys acquired imagery with 1-mm pixels that overcame the need to depend on subjective selection of "representative" study areas. Summarizing, aerial surveys acquiring multi-resolution imagery that includes 1-mm pixel data have repeatedly demonstrated:

1. Lower cost than extensive conventional ground sampling for areas greater than about 200 ha;
2. Practical acquisition of large sample numbers;
3. Reduced sample-collection time;
4. Collection of many samples within short phenological windows;
5. Creation of permanent records that may be examined any time in the future; and
6. Capability of capturing sub-meter details for detecting ecologically important changes.

Measurement of bare ground from 1-mm pixel images is just one example of the different indicators of rangeland health that may be monitored.

12.6.3 Visual Analysis

For measuring ground cover, image resolution should be at least 1-mm resolution (Booth and Cox, 2009). Attempts to accurately measure ground-cover from 10-, 20-, and 50-mm resolution imagery were unsuccessful (Booth and Cox, 2009; Duniway et al., 2012; Weber et al., 2013). Figure 12.8 shows that 1-mm resolution images are essential to capturing the detail needed for identifying species. Current methods for analysis of this type of imagery include visual-analysis-facilitating

FIGURE 12.8 Portion of a 3 × 4-m aerial image (0.9-mm pixel size) acquired from a light sport airplane traveling 84 km/h at an altitude of 103 m above ground level in the Red Desert of central Wyoming. The main image shows bare soil, litter, shadow, grasses, sagebrush (*Artemisia tridentata* Nutt.) and yellow rabbitbrush (*Chrysothamnus viscidiflorus* (Hook.) Nutt.), while the circular inset (circled area on main image enlarged twofold) shows goldenweed (*Stenotus acaulis* (Nutt.) Nutt.).

software programs (Booth et al., 2006a, 2006b). These programs are accurate when used with appropriate image resolutions (you can't measure what you can't see), and by people with adequate field experience.

SamplePoint is free software (available online at www.SamplePoint.org; last accessed 30 May 2014) that facilitates point sampling of digital images. Because the sample point is always a single pixel of the image (Figure 12.9a), where the spatial resolution is equal or less than 1 mm, the analysis has a potential accuracy of 92%. To use the program, images are loaded from a computer directory, and a database is created to store the data entered. The number and pattern of sample points (grid or random) are determined by the user (Figure 12.9b). The predetermined classes are associated with buttons along the bottom of the image. *SamplePoint* automatically moves from point to point when the class information is entered by clicking one of the buttons. The software allows image magnification (zoom), and it will support up to three monitors, each of which displays the image with different levels of magnification.

Images need not be orthorectified or georeferenced for use in SamplePoint. Thus, users with no GIS experience can use the software effectively. This is an important point because other point-sampling tools like Image Interpreter Tool (Duniway et al., 2012) and Digital Mylar (Clark et al., 2004; RSAC, 2014) do require georeferenced imagery. That adds a workflow step that makes the software more difficult and time-consuming to use for those who have GIS experience, and virtually impossible for those who don't. The cited tools function very well with orthoimagery, as intended. Nevertheless, for ground- or aerial-based photo plot monitoring, a georeferenced image prerequisite restricts usage of these tools because (1) it is impractical to georeference hundreds of disconnected plot-based images and (2) commercial sub-meter orthoimagery is too expensive to acquire frequently. To illustrate, over the last six years the Bureau of Land Management contracted

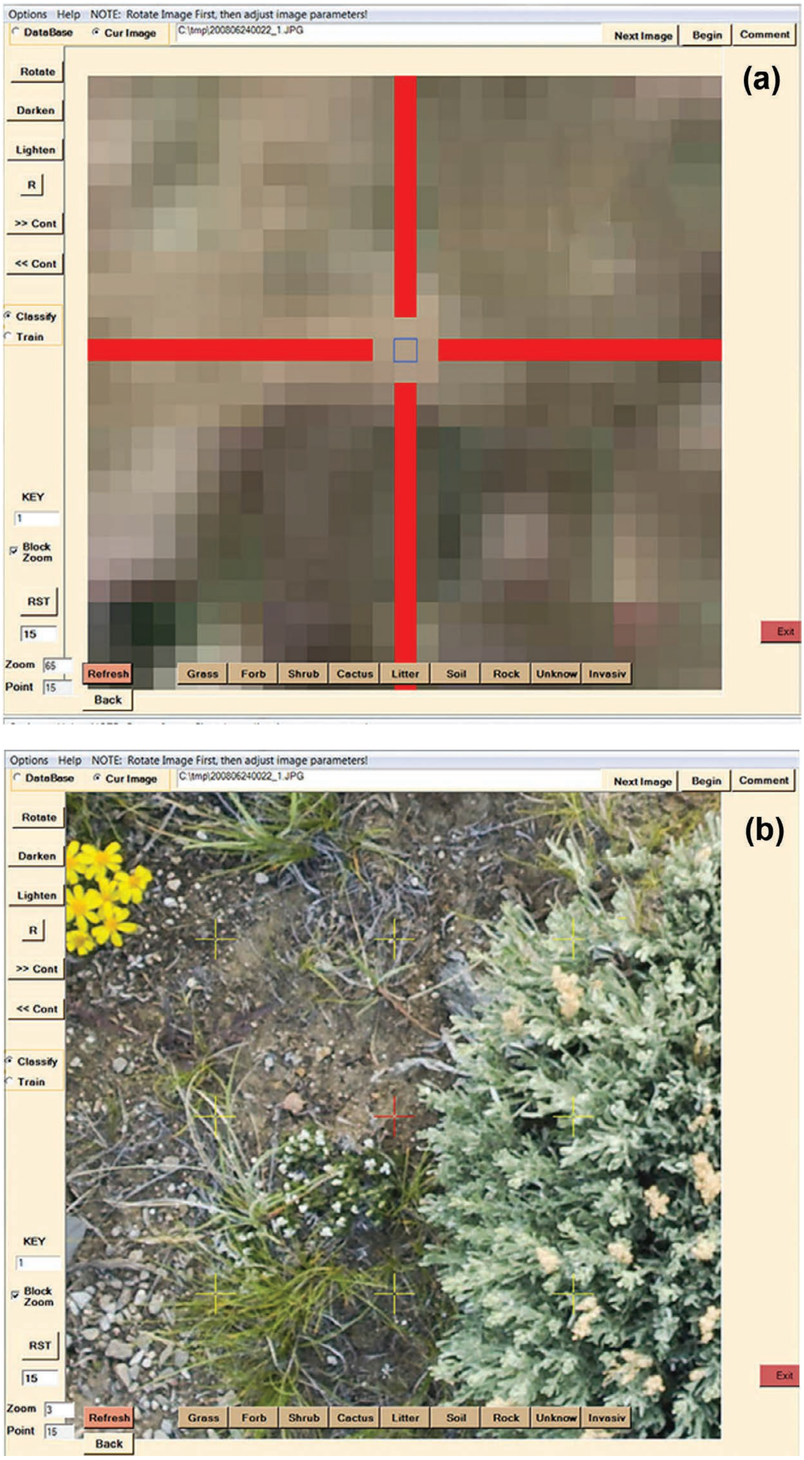

FIGURE 12.9 SamplePoint analysis of a ground photograph in Wyoming's Red Desert associated with aerial images (Figure 12.8) collected using the flight plan in Figure 12.7. Classification is performed on a single pixel within a 9-pixel array framed by the red crosshair by clicking one of the user-defined buttons along the bottom of the screen (a). The same sampling point is shown zoomed out (b) to show the context of the point that is hitting bare ground in between spiny phlox (*Phlox hoodii* Richardson) and sagebrush (*Artemesia tridentata* Nutt.). Note the systematic grid sampling pattern of the classification crosshairs.

only one sub-meter orthoimage collection in the state of Wyoming: 30-cm resolution at $18/km^2. Collection of the 2–3-cm orthoimagery that Duniway et al. (2012) reported as yielding reliable estimates for many cover types will cost substantially more than $18/km^2, limiting usage among agencies where even contracting for 30-cm orthoimagery is usually cost-prohibitive. As internal collection capabilities improve, cost may become less of a factor.

First-time users of 1-mm resolution imagery are often surprised at the number of species they can identify in an image. This leads to an initial presumption that they can use *SamplePoint* to measure cover by species. While this may be true for appropriately spaced woody species, measuring cover by plant functional type (grasses, grass-like plants, and forbs) is usually more practical except where and when plant species are distinctive. *SamplePoint* does *not* correct for user biases that may occur due to personal interpretations of protocol (e.g., what is litter), or correct for conditions such as age that can influence color perception. In fact, the variation among *SamplePoint* users was found to be about equal with that of users of the line-point intercept (Moffet, 2009). Additionally, multiple people used *SamplePoint* to analyze the same set of images showing there are user biases in class selection. When biases are found, the image dataset can be re-analyzed. Thus, data verifiability and the capability to significantly increase sampling are key advantages of using *SamplePoint* with image-based monitoring.

Two other programs are also freely available at www.SamplePoint.org, *SampleFreq* and *ImageMeasurement*. *SampleFreq* functions similarly to *SamplePoint*, but it facilitates nested frequency sampling. *ImageMeasurement* is used to measure areas and lengths from nadir imagery of known scale. Originally, this program was used to measure stream and channel widths with other ecological indicators for riparian areas. *ImageMeasurement* is unique among similar programs by incorporating exact image resolution for every image in a multi-image dataset.

12.6.4 Unmanned Aircraft Systems (UAS)

Unmanned aircraft systems (UAS) may also be effective platforms for remote sensing (Hardin and Jackson, 2005; Rango et al., 2006, 2009; Hardin and Hardin, 2010). Some of the first UAS that were used in agricultural and natural resource management were made from radio-control model aircraft (Parracciani et al., 2024; Fenetahun et al., 2022; Matongera et al., 2021; Tomlins and Lee, 1983; Quilter and Anderson, 2000, 2001). Now, there are many types of advanced civilian UAS, from high-altitude long-endurance to low-altitude short-endurance aircraft (Watts et al., 2012), so few generalizations may be made about current UAS flight capabilities. LSAs may fly in steady wind conditions of 32 km/h when there are no wind gusts. Two particular UAS (UX5 and Gatewing X100, Trimble Navigation Limited, Westminster, CO, USA) are claimed to be able to fly in 65 km/h winds (Trimble Navigation, 2013), because the automatic pilot updates aircraft controls at 100 Hz (Southard, 2013). The ability of UAS to fly in moderate to high winds may facilitate timely collection of aerial data for biodiversity.

Like manned aircraft, UAS may be configured with medium-resolution, high spectral resolution, or high spatial resolution sensors. Furthermore, LiDAR, thermal infrared, radar, and other sensors are available for UAS platforms. Most of the research uses small low-flying UAS with digital cameras to measure ground cover (Ocholla et al., 2024; Dube et al., 2021; McCord et al., 2017; Hardin et al., 2007; Laliberte et al., 2007, 2010; Breckenridge and Dakins, 2011; Breckenridge et al., 2011). Hardin et al. (2007) using small UAS to detect squarrose knapweed found that overall detection accuracy was low but the rate of false positives was miniscule. Breckenridge et al. (2011) also attempted to determine presence and sex of sage grouse (*Centrocercus urophasianus*) using decoys to represent grouse during spring mating season. At a height of 73 m, 100% of the male and 80% of the female decoys could be detected by a skilled observer, whereas at 305 m height, 90% of the male and only 10% of the female decoys could be detected by the skilled observer.

With small UAS and digital cameras, it is easy to acquire many more images than would be possible to analyze using aids such as *SamplePoint*, so automated processing or preprocessing is required.

Many people using these systems have backgrounds in image processing, in which the typical workflow would be production of orthorectified image mosaics. Two general methods used in orthorectification are the scale invariant feature transform (Lowe, 2004) and structure from motion (Turner et al., 2012; Westoby et al., 2012). Classification of land cover types from these image mosaics is not very accurate when using methods developed for multispectral satellite data, because the spectral properties of a small pixel have little connection with its cover type (Figure 12.6). Instead, the spatial relationships among pixels are used in an object-based classification (Parracciani et al., 2024; Retallack et al., 2023; Questad et al., 2022; Dube et al., 2021; McCord et al., 2017; Luscier et al., 2006; Laliberte et al., 2007, 2010; Laliberte and Rango, 2011).

12.6.5 Assessment of High Spatial Resolution

Remote sensing with high spatial resolution sensors can be used for monitoring numerous indicators of rangeland health (Table 12.1) in order to get a preponderance of evidence for evaluation. Aircraft are necessary for HSR data acquisition; and image analysis currently requires human inputs. The typical image-processing workflow for aerial photography is to geo- and ortho-rectify the large number of photographs to produce a single image with boundary-to-boundary coverage. We suggest that this time-consuming effort is not necessary for rangeland monitoring. By assuming each photograph is one plot in a statistical sample, accurate conclusions may be determined regarding the land area as a whole. Furthermore, from the geographic coordinates of each photograph, the plot-scale results may be combined for landscape-scale information by kriging or co-kriging.

Unsupervised or supervised classification of remote sensed imagery requires areas of a known category for training, which is a problem for early detection of invasive species. Computer-facilitated interpretation of HSR data may be used to detect plant species new to an area, because photographs from other areas would be used as examples. Furthermore, with low-cost data storage, HSR acquisitions may be archived for re-examination.

Most of the airborne HSR data used for method development were acquired using a manned light sport aircraft (Booth and Cox, 2009, 2011), and the costs for LSA remote sensing were less than other methods. The decade-long LSA effort included a strong emphasis on safety and there were no incidents during the thousands of LSA flight-hours. Even though the availability of high-quality components have made UAS much more reliable than a few years ago, there will be flight and control failures. The expanse of rangelands is large, so the number of flight hours required for monitoring will be large; using either LSA or UAS as low-altitude platforms should facilitate the acquisition of HSR imagery for rangeland monitoring.

12.7 CONCLUSIONS

Rangeland state-and-transition models account for differences in plant communities occurring at an ecological site, and these models are being adopted in different countries for rangeland management (Kouba et al., 2024; Ocholla et al., 2024; Parracciani et al., 2024; Angerer et al., 2023; Kleinhesselink et al., 2023; Retallack et al., 2023; Thornley et al., 2023; Fenetahun et al., 2022; Maphanga et al., 2022; Questad et al., 2022; Dube et al., 2021; Matongera et al., 2021; Sawalhah et al., 2018; Jafari et al., 2017; McCord et al., 2017). Based on the natural range of variation, recently disturbed ecological sites in the reference state may have lower diversity and biomass compared to an alternative state. Therefore, after accounting for interannual variation in precipitation, detecting lower biomass with spectral vegetation indices is not necessarily equal to detecting rangeland degradation. Instead, degraded rangelands crossed a transition into an alternative ecological state such that the area will not recover over time to its former diversity, biomass, and structure. Operational monitoring of rangelands by remote sensing needs to be based on the information required for management in order to prevent degradation.

As discussed in this chapter, there are many examples showing how sensors with different combinations of high spectral resolution, high temporal resolution, and high spatial resolution may be used to measure biodiversity, usually by detecting various indicators of rangeland health. We attempted to make the best possible case for rangeland monitoring with each data type. *At the current time, we conclude that facilitated image interpretation of high spatial resolution data is the best method for rangeland monitoring for management based on state-and-transition models.* This conclusion is based on one narrowly focused objective, providing information required for modifying management practices in order to protect rangeland diversity and prevent rangeland degradation. Other objectives, such as estimating biomass forage production, require other sources of remotely sensed data.

Medium resolution satellite data have been available for decades, and the only rangeland health indicator that may be reliably estimated is the amount of bare ground (Table 12.1). Transitions to alternative states may be recognized afterwards, but perhaps too late to prevent further degradation. High temporal resolution data from operational meteorological satellites are necessary for monitoring vegetation phenology, functional types, and effects of drought. Phenology using higher spatial resolution data from satellites currently in orbit is an extremely important new source of information, and there should be an international effort to archive these data for world-wide availability. Multiple years' worth of data need to have been acquired and available in order to account for interannual variability in temperature and precipitation.

High spectral resolution data may be used to detect and measure bare soil, many different invasive species, and most plant functional types, the three most important indicators of rangeland health (MacKinnon et al., 2011). Combined hyperspectral sensors and LiDAR in aircraft (Kouba et al., 2024; Ocholla et al., 2024; Parracciani et al., 2024; Angerer et al., 2023; Kleinhesselink et al., 2023; Retallack et al., 2023; Thornley et al., 2023; Fenetahun et al., 2022; Maphanga et al., 2022; Questad et al., 2022; Dube et al., 2021; Matongera et al., 2021; Sawalhah et al., 2018; Jafari et al., 2017; McCord et al., 2017; Asner et al., 2007; Asner and Martin, 2009; Kampe et al., 2010) are promising because it is much easier to identify pure spectral components. Airborne sensors have pixel sizes from 5 to 30 m, so image texture would help identify areas of spatial heterogeneity for animal habitat. Finally, litter cover, biological crusts, and forage quality may be determined by chemical composition.

Hyperspectral remote sensing does well when either the analyst has some prior information on where the target is located (such as invasive species) or the spectral signature is invariant (cellulose and lignin for litter cover). Soil minerals have spectral signatures, whereas soil types are classified based on pedogenesis. Plant species do not have signatures in the way that soil minerals and biological compounds do, but this conclusion is being re-evaluated using more-advanced airborne sensors (Asner and Martin, 2009, 2011; Asner et al., 2011). Furthermore, Rocchini et al. (2010a, 2010b) hypothesized spectral diversity *per se* is important for estimating biodiversity, which is parallel to the claim that spatial diversity from image texture is important for estimating biodiversity. Object-based classification combines both spectral and spatial diversity and may become an effective method.

Rangeland monitoring with high spatial resolution data provides information directly relevant for management based on rangeland health, to avoid transitions to more degraded states. There may be a large difference between the scales at which information is useful compared to the scales at which the data is acquired to produce the information. The scale for information required by rangeland managers is the landscape, but acquisition of high spatial resolution data may be the most cost effective method of obtaining the required information.

12.8 DISCLAIMER

Mention of product names is for information only, does not imply government endorsement and other products may be equally suitable.

REFERENCES

Adams, J. B., Smith, M. O., & Johnson, P. E. 1986. Spectral mixture modeling: A new analysis of rock and soil types at the Viking Lander 1 site. Journal of Geophysical Research, 91, 8098–8112.

Adelabu, S., Mutanga, O., Adam, E., & Cho, M. A. 2013. Exploiting machine learning algorithms for tree species classification in a semiarid woodland using RapidEye image. Journal of Applied Remote Sensing, 7, 073480–1.

Adjorlolo, C., Cho, M. A., Mutanga, O., & Ismail, R. 2012a. Optimizing spectral resolutions for the classification of C_3 and C_4 grass species, using wavelengths of known absorption features. Journal of Applied Remote Sensing, 6, 063560.

Adjorlolo, C., Mutanga, O., Cho, M. A., & Ismail, R. 2012b. Challenges and opportunities in the use of remote sensing for C_3 and C_4 grass species discrimination and mapping. African Journal of Range and Forage Science, 29, 47–61.

Allen, C. R., Gunderson, L., & Johnson, A. R. 2005. The use of discontinuities and functional groups to assess relative resilience in complex systems. Ecosystems, 8, 958–966.

Anderson, G. L., Carruthers, R. I., Ge, S., & Gong, P. 2005. Monitoring of invasive *Tamarix* distribution and effects of biological control with airborne hyperspectral remote sensing. International Journal of Remote Sensing, 26, 2487–2489.

Anderson, G. L., Everitt, J. H., Escobar, D. E., Spencer, N. R., & Andrascik, R. J. 1996. Mapping leafy spurge (*Euphorbia esula*) infestations using aerial photography and geographic information systems. Geocarto International, 11, 81–89.

Anderson, G. L., Prosser, C. W., Wendel, L. E., Delfosse, E. S., & Faust, R. M. 2003. The ecological area-wide management (TEAM) of leafy spurge program of the United States Department of Agriculture – Agricultural Research Service. Pest Management Science, 59, 609–613.

Anderson, R. P., Peterson, A. T., & Egbert, S. L. 2006. Vegetation-index models predict areas vulnerable to purple loosestrife (*Lythrum salicaria*) invasion in Kansas. Southwestern Naturalist, 51, 471–480.

Andrew, M. E., & Ustin, S. L. 2006. Spectral and physiological uniqueness of perennial pepperweed (*Lepidium latifolium*). Weed Science, 54, 1051–1062.

Andrew, M. E., & Ustin, S. L. 2008. The role of environmental context in mapping invasive plants with hyperspectral image data. Remote Sensing of Environment, 112, 4301–4317.

Andrew, M. E., & Ustin, S. L. 2009. Habitat suitability modeling of an invasive plant with advanced remote sensing data. Diversity and Distributions, 15, 627–640.

Angerer, J. P., Fox, W. E., Wolfe, J. E., Tolleson, D. R., & Owen, T. 2023. Chapter 20—Land degradation in rangeland ecosystems. Pages 394–434 in *Hazards and Disasters Series, Biological and Environmental Hazards, Risks, and Disasters* (Second Edition) (Ramesh Sivanpillai and John F. Shroder, eds.). Elsevier, ISBN 9780128205099, https://doi.org/10.1016/B978-0-12-820509-9.00007-1. (www.sciencedirect.com/science/article/pii/B9780128205099000071)

Asner, G. P. 2004. Biophysical remote sensing signatures of arid and semiarid ecosystems. Pages 53–109 in *Remote Sensing for Natural Resource Management and Environmental Monitoring. Manual of Remote Sensing, 3rd Edition, Volume 4* (S. L. Ustin, ed.). Hoboken, NJ: John Wiley and Sons.

Asner, G. P., Knapp, D. E., Kennedy-Bowdoin, T., Jones, M. O., Martin, R. E., Boardman, J., & Field, C. B. 2007. Carnegie airborne observatory: In-flight fusion of hyperspectral imaging and waveform light detection and ranging (wLiDAR) for three-dimensional studies of ecosystems. Journal of Applied Remote Sensing, 1, 013536.

Asner, G. P., & Martin, R. E. 2009. Airborne spectranomics: Mapping canopy chemical and taxonomic diversity in tropical forests. Frontiers in Ecology and Environment, 7, 269–276.

Asner, G. P., & Martin, R. E. 2011. Canopy phylogenetic, chemical and spectral assembly in a lowland Amazonian Forest. New Phytologist, 189, 999–1012.

Asner, G. P., Martin, R. E., Knapp, D. E., Tupayachi, R., Anderson, C., Carranza, L., Martinez, P., Houcheime, M., Sinca, F., & Weiss, P. 2011. Spectroscopy of canopy chemicals in humid tropical forests. Remote Sensing of Environment, 115, 3587–3598.

Balch, J. K., Bradley, B. A., D'Antonio, C. M., & Gómez-Dans, J. 2013. Introduced annual grass increases regional fire activity across the arid western USA. Global Change Biology, 19, 173–183.

Bastin, G. N., Denham, R., Scarth, P., Sparrow, A., & Chewings, V. 2014. Remotely-sensed analysis of ground-cover change in Queensland's rangelands, 1988–2005. Rangeland Journal, 36, 191–204.

Bastin, G. N., Scarth, P., Chewings, V., Sparrow, A., Denham, R., Schmidt, M., O'Reagain, P., Shepard, R., & Abbot, B. 2012. Separating grazing and rainfall effects at regional scale using remote sensing imagery: A dynamic reference-cover method. Remote Sensing of Environment, 121, 443–457.

Bastin, G. N., Stafford Smith, D. M., Watson, I. W., & Fisher, A. 2009. The Australian collaborative rangelands information system: Preparing for a climate of change. Rangeland Journal, 31, 111–125.

Belgacem, A. O., & Louhaichi, M. 2013. The vulnerability of native rangeland plant species to global climate change in the West Asia and North African regions. Climatic Change, 119, 451–463.

Bellis, L. M., Pidgeon, A. M., Radeloff, V. C., St-Louis, V., Navarro, J. L., & Martella, M. B. 2008. Modeling habitat suitability for greater rheas based on satellite image texture. Ecological Applications, 18, 1956–1966.

Bentivegna, D. J., Smeda, R. J., & Wang, C. 2012. Detecting cutleaf teasel (*Dipsacus laciniatus*) along a Missouri highway with hyperspectral imagery. Invasive Plant Science and Management, 5, 155–163.

Bestelmeyer, B. T. 2006. Threshold concepts and their use in rangeland management and restoration: The good, the bad, and the insidious. Restoration Ecology, 14, 325–329.

Bestelmeyer, B. T., Goolsby, D. P., & Archer, S. R. 2011. Spatial perspectives in state-and-transition models: A missing link to land management. Journal of Applied Ecology, 48, 746–757.

Blaschke, T. 2010. Object-based image analysis for remote sensing. ISPRS Journal of Photogrammetry and Remote Sensing, 65, 2–16.

Blumenthal, D. M., Booth, D. T., Cox, S. E., & Ferrier, C. E. 2007. Large-scale aerial images capture details of invasive plant populations. Rangeland Ecology & Management, 60, 523–528.

Blumenthal, D. M., Norton, A. P., Cox, S. E., Hardy, E. M., Liston, G. E., Kennaway, L., Booth, D. T., & Derner, J. D. 2012. *Linaria dalmatica* invades south-facing slopes and less grazed areas in grazing-tolerant mixed-grass prairie. Biological Invasions, 14, 395–404.

Boardman, J. W., & Kruse, F. A. 2011. Analysis of imaging spectrometer data using N-dimensional geometry and a mixture-tuned matched filter approach. IEEE Transactions on Geoscience and Remote Sensing, 49, 4138–4152.

Booth, D. T., & Cox, S. E. 2008. Image-based monitoring to measure ecological change in rangeland. Frontiers of Ecology and Management, 6, 185–190.

Booth, D. T., & Cox, S. E. 2009. Dual-camera, high-resolution aerial assessment of pipeline revegetation. Environmental Monitoring and Assessment, 158, 23–33.

Booth, D. T., & Cox, S. E. 2011. Art to science: Tools for greater objectivity in resource monitoring. Rangelands, 33(4), 27–34.

Booth, D. T., Cox, S. E., & Berryman, R. D. 2006a. Point sampling digital imagery with 'Samplepoint'. Environmental Monitoring and Assessment, 123, 97–108.

Booth, D. T., Cox, S. E., & Berryman, R. D. 2006b. Precision measurements from very-large scale aerial digital imagery. Environmental Monitoring and Assessment, 112, 293–307.

Booth, D. T., Cox, S. E., Louhaichi, M., & Johnson, D. E. 2004. Lightweight camera stand for close-to-earth remote sensing. *Journal of Range Management*, 57, 675–678.

Booth, D. T., Cox, S. E., Meilke, T., & Zuuring, H. R. 2008. Ground-cover measurements: Assessing correlation among aerial and ground-based measurements. Environmental Management, 42, 1091–1100.

Booth, D. T., Cox, S. E., & Teel, D. 2010. Aerial assessment of leafy spurge (*Euphorbia esula* L.) on Idaho's Deep Fire Burn. Native Plants Journal, 11, 327–339.

Booth, D. T., & Tueller, P. T. 2003. Rangeland management using remote sensing. Arid Land Research and Management, 17, 455–467.

Boryan, C., Yang, Z., Mueller, R., & Craig, M. 2011. Monitoring US agriculture: The US department of agriculture, national agricultural statistics service, cropland data layer program. Geocarto International, 26, 341–358.

Bradley, B. A. 2013. Remote detection of invasive plants: A review of spectral, textural and phenological approaches. Biological Invasions, DOI: 10.1007/s10530-013-0578-9.

Bradley, B. A., Blumenthal, D. M., Wilcove, D. S., & Ziska, L. H. 2009. Predicting plant invasions in an era of global change. Trends in Ecology and Evolution, 25, 310–318.

Bradley, B. A., & Mustard, J. F. 2005. Identifying land cover variability distinct from land cover change: Cheatgrass in the Great Basin. Remote Sensing of Environment, 94, 204–213.

Bradley, B. A., & Mustard, J. F. 2006. Characterizing the landscape dynamics of an invasive plant and risk of invasion using remote sensing. Ecological Applications, 16, 1132–1147.

Breckenridge, R. P., & Dakins, M. 2011. Evaluation of bare ground on rangelands using unmanned aerial vehicles: A case study. GIScience & Remote Sensing, 48, 74–85.

Breckenridge, R. P., Dakins, M., Bunting, S., Harbour, J. L., & White, S. 2011. Comparison of unmanned aerial vehicle platforms for assessing vegetation cover in sagebrush steppe ecosystems. Rangeland Ecology & Management, 64, 521–532.

Briske, D. D., Bestelmeyer, B. T., Stringham, T. K., & Shaver, P. L. 2008. Recommendations for development of resilience-based state-and-transition models. Rangeland Ecology & Management, 61, 359–367.

Briske, D. D., Fuhlendorf, S. D., & Smeins, F. E. 2005. State-and-transition models, thresholds, and rangeland health: A synthesis of ecological concepts and perspectives. Rangeland Ecology & Management, 58, 1–10.

Briske, D. D., Fuhlendorf, S. D., & Smeins, F. E. 2006. A unified framework for assessment and application of ecological thresholds. Rangeland Ecology & Management, 59, 225–236.

Brown, J. R.1994. State and transition models for rangelands. 2. Ecology as a basis for rangeland management: Performance criteria for testing models. Tropical Grasslands, 28, 206–213.

Brown, J. R. 2010. Ecological sites: Their history, status and future. Rangelands, 32(6), 5–8.

Cagney, J., Cox, S. E., & Booth, D. T. 2011. Comparison of point intercept and image analysis for monitoring rangeland transects. Rangeland Ecology & Management, 64, 309–315.

Carter, G. A., Knapp, A. K., Anderson, J. E., Hoch, G. A., & Smith, M. D. 2005. Indicators of plant species richness in AVIRIS spectra of a mesic grassland. Remote Sensing of Environment, 98, 304–316.

Carter, G. A., Lucas, K. L., Blossom, G. A., Lassitter, C. L., Holiday, D. M., Mooneyhan, D. S., Fastring, D. R., Holcombe, T. R., & Griffith, J. A. 2009. Remote sensing and mapping tamarisk along the Colorado River, USA: A comparative use of summer-acquired hyperion, thematic mapper, and quickbird data. Remote Sensing, 1, 318–329.

Caudle, D., Sanchez, H., DiBenedetto, J., Talbot, C., & Karl, M. 2013. *Interagency Ecological Site Handbook for Rangelands*. Washington, DC: US DOI Bureau of Land Management, USDA Forest Service, and USDA Natural Resource Conservation Service. http://www.ars.usda.gov/Research/docs.htm?docid=18502, last accessed 28 Feb. 2014.

Chang, C.-I. 2000. An information-theoretic approach to spectral variability, similarity, and discrimination for hyperspectral image analysis. IEEE Transactions on Information Theory, 46, 1927–1932.

Cheng, Y. B., Tom, E., & Ustin, S. L. 2007. Mapping an invasive species, kudzu (*Pueraria montana*), using hyperspectral imagery in western Georgia. Journal of Applied Remote Sensing, 1, 013514.

Cho, M. A., Debba, P., Mathieu, R., Naidoo, L., van Aardt, J., & Asner, G. P. 2010. Improving discrimination of savanna tree species through a multiple-endmember spectral angle mapper approach: Canopy level analysis. IEEE Transactions on Geoscience and Remote Sensing, 48, 4133–4142.

Clark, J., Finco, M., Warbington, R., & Schwind, B. 2004. Digital Mylar: A tool to attribute vegetation polygon features over high-resolution imagery. In: *Proceedings of the Tenth Forest Service Remote Sensing Applications Conference* Salt Lake City, Utah. www.fs.fed.us/r5/rsl/publications/, last accessed 9 March 2014.

Clark, M. L., Roberts, D. A., & Clark, D. B. 2005. Hyperspectral discrimination of tropical rainforest tree species at leaf to crown scales. Remote Sensing of Environment, 96, 375–398.

Clark, R. N., Swayze, G. A., Livo, K. E., Kokaly, R. F., Sutley, S. J., Dalton, J. B., McDougal, R. R., & Gent, C. A. 2003. Imaging spectroscopy: Earth and planetary remote sensing with the USGS Tetracorder and expert systems. Journal of Geophysical Research, 108, E12, 5131.

Clements, F. E. 1916. *Plant Succession:An Analysis of the Development of Vegetation*. Carnegie Institute Publication Volume 242. Washington, DC: Carnegie Institute of Washington.

Clinton, N. E., Potter, C., Crabtree, B., Genovese, V., Gross, P., & Gong, P. 2010. Remote sensing-based time-series analysis of cheatgrass (*Bromus tectorum* L.) phenology. Journal of Environmental Quality, 39, 955–963.

Congalton, R. G., & Green, K. 2008. *Assessing the Accuracy of Remotely Sensed Data: Principles and Practices*. Boca Raton, FL: CRC press, Taylor and Francis Group, 183 pp.

Cooper, W. S. 1924. An apparatus for photographic recording of quadrats. Journal of Ecology, 12, 317–321.

Culbert, P. D., Radeloff, V. C., St-Louis, V., Flather, C. H., Rittenhouse, C. D., Albright, T. P., & Pidgeon, A. M. 2012. Modeling broad-scale patterns of avian species richness across the Midwestern United States with measures of satellite image texture. Remote Sensing of Environment, 118, 140–150.

Dalmayne, J., Möckel, T., Prentice, H. C., Schmid, B. C., & Hall, K. 2013. Assessment of fine-scale plant species beta diversity using WorldView-2 satellite spectral dissimilarity. Ecological Informatics, 18, 1–9.

Daughtry, C. S. T. 2001. Discriminating crop residues from soil by shortwave infrared reflectance. Agronomy Journal, 93, 125–131.

Daughtry, C. S. T., & Hunt Jr., E. R. 2008. Mitigating the effects of soil and residue water contents on remotely sensed estimates of crop residue cover. Remote Sensing of Environment, 112, 1647–1657.

Davidson, A., & Csillag, F. 2001. The influence of vegetation index and spatial resolution on a two-date remote sensing-derived relation to C4 species coverage. Remote Sensing of Environment, 75, 138–151.

Davidson, E. A., Asner, G. P., Stone, T. A., Neill, C., & Figueiredo, R. O. 2008. Objective indicators of pasture degradation from spectral mixture analysis of Landsat imagery. Journal of Geophysical Research, 113, G00B03.

de Beurs, K. M., & Henebry, G. M. 2004. Land surface phenology, climatic variation, and institutional change: Analyzing agricultural land cover change in Kazakhstan. Remote Sensing of Environment, 89, 497–509.

de Beurs, K. M., & Henebry, G. M. 2010. Spatio-temporal statistical methods for modeling land surface phenology. Pages 177–208 in *Phenological Research* (I. L. Hudson and M. R. Keatley, eds.). New York, NY: Springer Science and Business Media.

DiTomaso, J. M. 2000. Invasive weeds in rangelands: Species, impacts, and management. Weed Science, 48, 255–265.

Dobowski, S. Z., Safford, H. D., Cheng, Y. B., & Ustin, S. L. 2008. Mapping mountain vegetation using species distribution modeling, image-based texture analysis, and object-based classification. Applied Vegetation Science, 11, 499–508.

Dube, T., Shoko, C. and Gara, T. W. 2021. Remote sensing of aboveground grass biomass between protected and non-protected areas in savannah rangelands. African Journal of Ecology, Wiley online library. 59:3, 687–695.

Dudek, K. B., Root, R. R., Kokaly, R. F., & Anderson, G. L. 2004. Increased spatial and temporal consistency of leafy spurge maps from multidate AVIRIS imagery: A modified, hybrid linear spectral mixture analysis/mixture-tuned matched filtering approach. In *Proceedings of the 13th JPL Airborne Earth Science Workshop* (R. O. Green, ed.). Pasadena, CA, USA: Jet Propulsion Laboratory.

Duniway, M. C., Karl, J. W., Schrader, S., Baquera, N., & Herrick, J. E. 2012. Range and pasture monitoring using high resolution aerial imagery: A repeatable image interpretation approach. Environmental Monitoring and Assessment, 184, 789–804.

Elmqvist, T., Folke, C., Nyström, M., Peterson, G., Bengtsson, J., Walker, B., & Norberg, J. 2003. Response diversity, ecosystem change, and resilience. Frontiers of Ecology and Management, 1, 488–494.

Eyre, T. J., Fisher, A., Hunt, L. P., & Kutt, A. S. 2011a. Measure it to better manage it: A biodiversity monitoring framework for the Australian rangelands. Rangeland Journal, 33, 239–253.

Eyre, T. J., Kelly, A. L., Neldner, V. J., Wilson, B. A., Ferguson, D. J., Laidlaw, M. J., & Franks, A. J. 2011b. *BioCondition: A Condition Assessment Framework for Terrestrial Biodiversity in Queensland*. Assessment Manual. Version 2.1. Brisbane, Queensland, Australia: Department of Environment and Resource Management (DERM), Biodiversity and Ecosystem Sciences.

Fenetahun, Y., Yuan, Y., Xu, X., Wang, Y. 2022. Borana rangeland of southern Ethiopia: Estimating biomass production and carrying capacity using field and remote sensing data. Plant Diversity, 44:6, 598–606, ISSN 2468–2659, https://doi.org/10.1016/j.pld.2022.03.003. (www.sciencedirect.com/science/article/pii/S2468265922000361)

Feret, J. B., François, C., Asner, G. P., Gitelson, A. A., Martin, R. E., Bidel, L. P. R., Ustin, S. L., le Maire, G., & Jaquemoud, S. 2008. PROSPECT-4 and 5: Advances in the leaf optical properties model separating photosynthetic pigments. Remote Sensing of Environment, 112, 3030–3043.

Fletcher, R. S., Everitt, J. H., & Yang, C. 2011. Identifying saltcedar with hyperspectral data and support vector machines. Geocarto International, 26, 195–209.

Folke, C., Carpenter, S., Walker, B., Scheffer, M., Elmqvist, T., Gunderson, L., & Holling, C. S. 2004. Regime shifts, resilience, and biodiversity in ecosystem management. Annual Review of Ecology, Evolution, and Systematics, 35, 557–581.

Foody, G. M., & Dash, J. 2007. Discriminating and mapping the C3 and C4 composition of grasslands in the northern Great Plains, USA. Ecological Informatics, 2, 89–93.

Foody, G. M., & Dash, J. 2010. Estimating the relative abundance of C_3 and C_4 grasses in the Great Plains from multi-temporal MTCI data: Issues of compositing period and spatial generalizability. International Journal of Remote Sensing, 31, 351–362.

Franklin, S. E. 2010. *Remote Sensing for Biodiversity and Wildlife Management*. New York: McGraw-Hill, 346 pp.

Franklin, S. E., & Wulder, M. A. 2002. Remote sensing methods in medium spatial resolution satellite data land cover classification of large areas. Progress in Physical Geography, 26, 173–205.

Friedl, M. A., Sulla-Menashe, D., Tan, B., Schnieder, A., Ramankutty, N., Sibley, A., & Huang, X. 2010. MODIS collection 5 global land cover: Algorithm refinements and characterization of new datasets. Remote Sensing of Environment, 114, 168–182.

Fuhlendorf, S. D., & Engle, D. M. 2001. Restoring heterogeneity on rangelands: Ecosystem management based on evolutionary grazing patterns. Bioscience, 51, 625–632.

Fuhlendorf, S. D., Harrell, W. C., Engle, D. M., Hamilton, R. G., Davis, C. A., & Leslie Jr., D. M. 2006. Should heterogeneity be the basis for conservation? Grassland bird response to fire and grazing. Ecological Applications, 16, 1706–1716.

Gao, B. C., Heidebrecht, K. B., & Goetz, A. F. H. 1993. Derivation of scaled surface reflectances from AVIRIS data. Remote Sensing of Environment, 44, 145–163.

Gaston, K. J. 2000. Global patterns in biodiversity. Nature, 405, 220–227.

Ge, S., Everitt, J., Carruthers, R., Gong, P., & Anderson, G. 2006. Hyperspectral characteristics of canopy components and structure for phonological assessment of an invasive weed. Environmental Monitoring and Assessment, 120, 109–126.

Ge, S., Xu, M., Anderson, G. L., & Carruthers, R. I. 2007. Estimating yellow starthistle (*Centaurea solstitialis*) leaf area index and aboveground biomass with the use of hyperspectral data. Weed Science, 55, 671–678.

Gibbons, P., Briggs, S. V., Ayers, D. A., Doyle, S., Seddon, J., McElhinny, C., Jones, N., Sims, R., & Doody, J. S. 2008. Rapidly quantifying reference conditions in modified landscapes. Biological Conservation, 141, 2483–2493.

Gibbons, P., Briggs, S. V., Ayers, D. A., Seddon, J., Doyle, S., Cosier, P., McElhinny, C., Pelly, V., & Roberts, K. 2009. An operational method to assess impacts of land clearing on terrestrial biodiversity. Ecological Indicators, 9, 26–40.

Gill, T. K., & Phinn, S. R. 2008. Estimates of bare ground and vegetation cover from Advanced Spaceborne Thermal Emission and Reflection Radiometer (ASTER) short-wave-infrared reflectance imagery. Journal of Applied Remote Sensing, 2, 023511.

Gillespie, T. W., Foody, G. M., Rocchini, D., Giorgi, A. P., & Saatchi, S. 2008. Measuring and modeling biodiversity from space. Progress in Physical Geography, 32, 203–221.

Glenn, N. F., Mundt, J. T., Weber, K. T., Prather, T. S., Lass, L. W., & Pettingill, J. 2005. Hyperspectral data processing for repeat detection of small infestations of leafy spurge. Remote Sensing of Environment, 95, 399–412.

Goodin, D. G., & Henebry, G. M. 1997. A technique for monitoring ecological disturbance in tallgrass prairie using seasonal NDVI trajectories and a discriminant function mixture model. Remote Sensing of Environment, 61, 270–278.

Gottschalk, T. K., Huettmann, F., & Ehlers, M. 2005. Thirty years of analyzing and modeling avian habitat relationships using satellite imagery data: A review. International Journal of Remote Sensing, 26, 2631–2656.

Gould, W. 2000. Remote sensing of vegetation, plant species richness, and regional biodiversity hotspots.
Ecological Applications, 10, 1861– 1870.

Goward, S. N., Chander, G., Pagnutti, M., Marx, A., Ryan, R., Thomas, N., & Tetrault, R. 2012. Complementarity of ResourceSat-1 AWiFS and Landsat TM/ETM+ sensors. Remote Sensing of Environment, 123, 41–56.

Green, R. O., Eastwood, M. L., Sarture, C. M., Chrien, T. G., Aronsson, M., Chippendale, B. J., Faust, J. A., Pavri, B. E., Chovit, C. J., Solis, M., Olah, M. R., & Williams, O. 1998. Imaging Spectroscopy Environment, 65, 227–248.

Gu, Y., B´elair, S., Mahfouf, J., & Deblonde, G. 2006. Optional interpolation analysis of leaf area index using MODIS data. Remote Sensing of Environment, 104, 283–96.

Gu, Y., Brown, J. F., Miura, T., van Leeuwen, W. J. D., & Reed, B. C. 2010. Phenological classification of the United States: A geographic framework for extending multi-sensor time-series data. Remote Sensing, 2, 526–544.

Guerschman, J. P., Hill, M. J., Renzullo, L. J., Barrett, D. J., Marks, A. S., & Botha, E. J. 2009. Estimating fractional cover of photosynthetic vegetation, non-photosynthetic vegetation and bare soil in the Australian tropical savanna region upscaling the EO-1 Hyperion and MODIS sensors. Remote Sensing of Environment, 113, 928–945.

Guo, X., Price, K. P., & Stiles, J. 2003. Grasslands discriminant analysis using Landsat TM single and multitemporal data. Photogrammetric Engineering & Remote Sensing, 69, 1255–1262.

Hall, K., Reitalu, T., Sykes, M. T., & Prentice, H. C. 2012. Spectral heterogeneity of QuickBird satellite data is related to fine-scale plant species spatial turnover in semi-natural grasslands. Applied Vegetation Science, 15, 145–157.

Hamada, Y., Stow, D. A., Coulter, L. L., Jafolla, J. C., & Hendricks, L. W. 2007. Detecting Tamarisk species (*Tamarix* spp.) in riparian habitats of Southern California using high spatial resolution hyperspectral imagery. Remote Sensing of Environment, 109, 237–248.

Haralick, R. M., Shanmugam, K., & Dinstein, I. 1973. Textural features for image classification. IEEE Transactions on Systems, Man and Cybernetics, 3, 610–621.

Hardin, P. J., & Hardin, T. J. 2010. Small-scale remotely piloted vehicles in environmental research. Geography Compass, 4:9, 1297–1311.

Hardin, P. J., & Jackson, M. W. 2005. An unmanned aerial vehicle for rangeland photography. Rangeland Ecology & Management, 58, 439–442.

Hardin, P. J., Jackson, M. W., Anderson, V. J., & Johnson, R. 2007. Detecting squarrose knapweed (*Centaurea virgata* Lam. ssp. *squarrosa* Gugl.) using a remotely piloted vehicle: A Utah case study. GIScience & Remote Sensing, 44, 203–219.

He, K. S., Rocchini, D., Neteler, M., & Nagendra, H. 2011. Benefits of hyperspectral remote sensing for tracking plant invasions. Diversity and Distributions, 17, 381–392.

Hernandez, A. J., & Ramsey, R. D. 2013. A landscape similarity index: Multitemporal remote sensing to track changes in big sagebrush ecological sites. Rangeland Ecology & Management, 66, 71–81.

Herrick, J. E., Van Zee, J. W., Havstad, K. M., Burkett, L. M., & Whitford, W. G. 2005a. *Monitoring Manual for Grassland, Shrubland, and Savanna Ecosystems, Volume I: Quick Start*. Las Cruces, NM: USDA-ARS Jornada Experimental Range. 36 pp.

Herrick, J. E., Van Zee, J. W., Havstad, K. M., Burkett, L. M., & Whitford, W. G. 2005b. *Monitoring Manual for Grassland, Shrubland, and Savanna Ecosystems, Volume II: Design, supplementary methods and interpretation*. Las Cruces, NM: USDA-ARS Jornada Experimental Range, 200 pp.

Hestir, E. L., Khanna, S., Andrew, M. E., Santos, M. J., Viers, J. H., Greenberg, J. A., Rajapakse, S. S., & Ustin, S. L. 2008. Identification of invasive vegetation using hyperspectral remote sensing in the California Delta ecosystem. Remote Sensing of Environment, 112, 4034–4047.

Higley, B. M., & Kelly, D. E. 1873. Home on the range. Kansas: Smith County Pioneer.

Homer, C., Huang, C., Yang, L., Wylie, B., & Coan, M. 2004. Development of a 2001 National Landcover Database for the United States. Photogrammetric Engineering & Remote Sensing, 70, 829–840.

Hooper, D. U., Chapin III, F. S., Ewel, J. J., Hector, A., Inchausti, P., Lavorel, S., Lawton, J. H., Lodge, D. M., Loreau, M., Naeem, S., Schmid, B., Setälä, H., Symstad, A. J., Vandermeer, J., & Wardle, D. A. 2005. Effects of biodiversity on ecosystem functioning: A consensus of current knowledge. Ecological Monographs, 75, 3–35.

Huang, C., & Asner, G. P. 2009. Applications of remote sensing to alien invasive plant studies. Sensors, 9, 4869–4889.

Huang, C., & Geiger, E. L. 2008. Climate anomalies provide opportunities for large-scale mapping of non-native plant abundance in desert grasslands. Diversity and Distributions, 14, 875–884.

Huang, C., Geiger, E. L., van Leeuven, W. J. D., & Marsh, S. E. 2009. Discrimination of invaded and native species sites in a semi-desert grassland using MODIS multi-temporal data. International Journal of Remote Sensing, 30, 897–917.

Huete, A. R. 1988. A soil-adjusted vegetation index (SAVI). Remote Sensing of Environment, 25, 295–309.

Huete, A. R., Didan, K., Miura, T., Rodriguez, E. P., Gao, X., & Ferreira, L. G. 2002. Overview of the radiometric and biophysical performance of the MODIS vegetation indices. Remote Sensing of Environment, 83, 195–213.

Hunt Jr., E. R., Daughtry, C. S. T., Kim, M. S., & Parker Williams, A. E. 2007. Using canopy reflectance models and spectral angles to assess potential of remote sensing to detect invasive weeds. *Journal of Applied Remote Sensing*, 1: 013506.

Hunt Jr., E. R., Everitt, J. H., Ritchie, J. C., Moran, M. S., Booth, D. T., Anderson, G. L., Clark, P. E., & Seyfried, M. S. 2003. Applications and research using remote sensing for rangeland management. Photogrammetric Engineering & Remote Sensing, 69, 675–693.

Hunt Jr., E. R., Gillham, J. H., & Daughtry, C. S. T. 2010. Improving potential geographic distribution models for invasive plants by remote sensing. Rangeland Ecology & Management, 63, 505–513.

Hunt Jr., E. R., McMurtrey III, J. E., Parker Williams, A. E., & Corp, L. A. 2004. Spectral characteristics of leafy spurge (*Euphorbia esula*) leaves and flower bracts. Weed Science, 52, 492–497.

Hunt Jr., E. R., & Parker Williams, A. E. 2006. Detection of flowering leafy spurge with satellite multispectral imagery. Rangeland Ecology & Management, 59, 494–499.

Irisarri, J. G. N., Oesterheld, M., Vernón, S. R., & Paruelo, J. M. 2009. Grass species differentiation through canopy hyperspectral reflectance. International Journal of Remote Sensing, 30, 5959–5975.

Jacquemoud, S., Ustin, S. L., Verdebout, J., Schmuck, G., Andreoli, G., & Hosgood, B. 1996. Estimating leaf biochemistry using the PROSPECT leaf optical properties model. Remote Sensing of Environment, 56, 194–202.

Jacquemoud, S., Verhoef, W., Baret, F., Bacour, C., Zarco-Tejada, P. J., Asner, G. P., François, C., & Ustin, S. L. 2009. PROSPECT+SAIL models: A review of use for vegetation characterization. Remote Sensing of Environment, 113(suppl), S56–S66.

Jafari, F., Jafari, R., & Bashari, H. 2017. Assessing the performance of remotely sensed landscape function indices in semi-arid rangelands of Iran. The Rangeland Journal, 39, 253–262.

Janetos, A., Hansen, L., Inouye, D., Kelly, B. P., Meyerson, L., Peterson, B., & Shaw, R. 2008. Chapter 5. Biodiversity. Pages 151–182 in: *The Effects of Climate Change on Agriculture, Land Resources, Water Resources, and Biodiversity in the United States*. Synthesis and Assessment Product 4.3. Washington, DC: U.S. Climate Change Science Program and the Subcommittee on Global Change Research.

Jiang, Z., Huete, A. R., Chen, J., Chen, Y., Li, J., Yan, G., & Zhang, X. 2006. Analysis of NDVI and scaled difference vegetation index retrievals of vegetation fraction. Remote Sensing of Environment, 101, 366–378.

Johansen, K., & Phinn, S. 2006. Mapping structure parameters and species composition of riparian vegetation using IKONOS and Landsat ETM+ data in Australian tropical savannahs. Photogrammetric Engineering & Remote Sensing, 72, 71–80.

John, R., Chen, J., Lu, N., Guo, K., Liang, C., Wei, Y., Noormets, A., Ma, K., & Han, X. 2008. Predicting plant diversity based on remote sensing products in the semi-arid region of Inner Mongolia. Remote Sensing of Environment, 112, 2018–2032.

Jönsson, P., & Eklundh, L. 2004. TIMESAT—A program for analyzing time-series of satellite sensor data. Computers & Geoscience, 30, 833–845.

Joyce, L. A., Briske, D. D., Brown, J. R., Polley, H. W., McCarl, B. A., & Bailey, D. W. 2013. Climate change and North American Rangelands: Assessment of mitigation and adaption strategies. Rangeland Ecology & Management, 66, 512–528.

Kampe, T. U., Johnson, B. R., Kuester, M., & Keller, M. 2010. NEON: The first continental-scale observatory with airborne remote sensing of vegetation biochemistry and structure. Journal of Applied Remote Sensing, 4, 043510.

Karnieli, A., Kokaly, R. F., West, N. E., & Clark, R. N. 2003. Remote sensing of biological soil crusts. Pages 431–455 in *Biological Soil Crusts: Structure,Function, and Management* (J. Belnap and O. L. Lange, eds.). Ecological Studies Volume 150. Berlin, Germany: Springer-Verlag.

Kleinhesselink, A. R., Kachergis, E. J., McCord, S. E., Shirley, J., Hupp, N. R., Walker, J., Carlson, J. C., Morford, S. L., Jones, M. O., Smith, J. T., Allred, B. W., Naugle, D. E., 2023. Long-term trends in vegetation on bureau of land management rangelands in the Western United States. Rangeland Ecology & Management, 87, 1–12, ISSN 1550–7424, https://doi.org/10.1016/j.rama.2022.11.004. (www.sciencedirect.com/science/article/pii/S1550742422001075)

Knox, N. M., Skidmore, A. K., Prins, H. H. T., Asner, G. P., van der Werff, H., de Boer, W. F., van der Waal, C., de Knegt, H. J., Kohi, E. M., Slotow, R., & Grant, R. C. 2011. Dry season mapping of savanna forage quality, using the hyperspectral Carnegie Airborne Observatory sensor. Remote Sensing of Environment, 115, 1478–1488.

Kogan, F., Gitelson, A., Zakarin, E., Spivak, L., & Lebed, L. 2003. AVHRR-based spectral vegetation index for quantitative assessment of vegetation state and productivity: Calibration and validation. Photogrammetric Engineering & Remote Sensing, 69, 899–906.

Kouba, Y., Doghbage, A., Merdas, S., & Bagousse-Pinguet, Y. E. 2024. Grazing exclusion modulates the effects of different components of plant diversity on biomass production in semiarid rangeland. Agriculture, Ecosystems & Environment, 365, 108914, ISSN 0167–8809, https://doi.org/10.1016/j.agee.2024.108914. (www.sciencedirect.com/science/article/pii/S016788092400032X)

Kremer, R. G., & Running, S. W. 1993. Community type differentiation using NOAA/AVHRR data within a sagebrush-steppe ecosystem. Remote Sensing of Environment, 46, 311–318.

Kruse, F. A., Lefkoff, A. B., Boardman, J. W., Heidebrecht, K. B., Shapiro, A. T., Barloon, P. J., & Goetz, A. F. H. 1993. The Spectral Image Processing System (SIPS)—interactive visualization and analysis of imaging spectrometer data. Remote Sensing of Environment, 44, 145–163.

Kumar, L., Sinha, P., Brown, J. F., Ramsey, R. D., Rigge, M., Stam, C. A., Hernandez, A. J., Hunt, E. R., & Reeves, M. C. In press. Rangeland, grassland, shrublands monitoring: Methods and approaches. Chapter 12 in *Remote Sensing Handbook.Volume II: Land Resources: Monitoring, Modeling, and Mapping* (P. S. Thenkabail, ed.). Boca Raton, FL: CRC Press Taylor & Francis Group.

Laliberte, A. S., Herrick, J. E., Rango, A., & Winters, C. 2010. Acquisition, orthorectification, and object-based classification of unmanned aerial vehicle (UAV) imagery for rangeland monitoring. Photogrammetric Engineering & Remote Sensing, 76, 661–672.

Laliberte, A. S., & Rango, A. 2011. Image processing and classification procedures for analysis of sub-decimeter imagery acquired with an unmanned aircraft over arid rangelands. GIScience & Remote Sensing, 48, 4–23.

Laliberte, A. S., Rango, A., Herrick, J. E., Fredrickson, E. L., & Burkett, L. 2007. An object-based image analysis approach for determining fractional cover of senescent and green vegetation with digital plot photography. Journal of Arid Environments, 69, 1–14.

Lass, L. W., Prather, T. S., Glenn, N. F., Weber, K. T., Mundt, J. T., & Pettingill, J. 2005. A review of remote sensing of invasive weeds and example of the early detection of spotted knapweed (*Centaurea maculosa*) and babysbreath (*Gypsophila paniculata*) with a hyperspectral sensor. Weed Science, 53, 242–251.

Lass, L. W., Thill, D. C., Shafii, B., & Prather, T. S. 2002. Detecting spotted knapweed (*Centaurea maculosa*) with hyperspectral remote sensing technology. Weed Technology, 16, 426–432.

Lavergne, S., Mouquet, N., Thuiller, W., & Ronce, O. 2010. Biodiversity and climate change: Integrating evolutionary and ecological responses of species and communities. Annual Review of Ecology, Evolution, and Systematics, 41, 321–350.

Lawrence, R. L., Wood, S. D., & Sheley, R. L. 2006. Mapping invasive plants using hyperspectral imagery and Breiman Cutler classifications (Random Forest). Remote Sensing of Environment, 100, 356–362.

Lesica, P., & Hanna, D. 2009. Effect of biological control on leafy spurge (*Euphorbia esula*) and diversity of associated grasslands over 14 years. Invasive Plant Science and Management, 2, 151–157.

Leyequien, E., Verrelst, J., Slot, M., Schaepman-Strub, G., Heitkönig, I. M. A., & Skidmore, A. 2007. Capturing the fugitive: Applying remote sensing to terrestrial animal distribution and diversity. International Journal of Applied Earth Observation and Geoinformation, 9, 1–20.

Louhaichi, M., Johnson, M. D., Woerz, A. L., Jasra, A. W., & Johnson, D. E. 2010. Digital charting technique for monitoring rangeland vegetation cover at local scale. International Journal of Agriculture and Biology, 12, 406–410.

Loveland, T. R., Merchant, J. W., Ohlen, D. O., & Brown, J. F. 1991. Development of a land-cover characteristics database for the conterminous U.S. Photogrammetric Engineering & Remote Sensing, 57, 1453–1463.

Lowe, D. G. 2004. Distinctive image features from scale-invariant keypoints. International Journal of Computer Vision, 60, 91–110.

Lu, D., & Weng, Q. 2007. A survey of image classification methods and techniques for improving classification performance. International Journal of Remote Sensing, 28, 823–870.

Ludwig, J. A., Bastin, G. N., Chewings, V. H., Eager, R. W., & Liedloff, A. C. 2007. Leakiness: A new index for monitoring the health of arid and semiarid landscapes using remotely sensed vegetation cover and elevation data. Ecological Indicators, 7, 442–454.

Ludwig, J. A., Eager, R. W., Bastin, G. N., Chewings, V. H., & Liedloff, A. C. 2002. A leakiness index for assessing landscape function using remote sensing. Landscape Ecology, 17, 157–171.

Ludwig, J. A., Eager, R. W., Liedloff, A. C., Bastin, G. N., & Chewings, V. H. 2006. A new landscape leakiness index based on remotely sensed ground-cover data. Ecological Indicators, 6, 327–336.

Ludwig, J. A., Tongway, D. J., Bastin, G. N., & James, C. D. 2004. Monitoring ecological indicators of rangeland functional integrity and their relation to biodiversity at local and regional scales. Austral Ecology, 29, 108–120.

Ludwig, J. A., Wiens, J. A., & Tongway, D. J. 2000. A scaling rule for landscape patches and how it applies to conserving soil resources in savannas. Ecosystems, 3, 84–97.

Luscier, J. D., Thompson, W. L., Wilson, J. M., Gorham, B. E., & Dragut, L. D. 2006. Using digital photographs and object-based image analysis to estimate percent ground cover in vegetation plots. Frontiers of Ecology and Management, 4, 408–413.

Lym, R. G. 2005. Integration of biological control agents with other weed management technologies: Success from the leafy spurge (*Euphorbia esula*) IPM program. Biological Control, 35, 366–375.

MacKinnon, W. C., Karl, J. W., Toevs, G. R., Taylor, J. J., Karl, M., Spurrier, C. S., & Herrick, J. E. 2011. *BLM Core Terrestrial Indicators and Methods*. Tech Note 440. Denver, CO: U.S. Department of the Interior, Bureau of Land Management, National Operations Center.

Madden, M. 2004. Remote sensing and geographic information system operations for vegetation mapping of invasive exotics. Weed Technology, 18, 1457–1463.

Mansour, K., & Mutanga, O. 2012. Classifying increaser species as an indicator of different levels of rangeland degradation using WorldView-2 imagery. Journal of Applied Remote Sensing, 6, 063558–1.

Mansour, K., Mutanga, O., & Everson, T. 2012. Remote sensing based indicators of vegetation species for assessing rangeland degradation: Opportunities and challenges. African Journal of Agricultural Research, 7, 3261–3270.

Maphanga, T., Dube, T., Shoko, C., & Sibanda, M. 2022. Advancements in the satellite sensing of the impacts of climate and variability on bush encroachment in savannah rangelands. Remote Sensing Applications: Society and Environment, 25, 100689, ISSN 2352–9385, https://doi.org/10.1016/j.rsase.2021.100689. (www.sciencedirect.com/science/article/pii/S2352938521002251)

Marsett, R. C., Qi, J., Heilman, P., Biedenbender, S. H., Watson, M. C., Amer, S., Weltz, M., Goodrich, D., & Marset, R. 2006. Remote sensing for grassland management in the arid southwest. Rangeland Ecology & Management, 59, 530–540.

Martin, M. P., Barreto, L., Riaño, D., Fernandez-Quintanilla, C., & Vaughan, P. 2011. Assessing the potential of hyperspectral remote sensing for the discrimination of grass weeds in winter cereal crops. International Journal of Remote Sensing, 31, 49–67.

Matongera, T. N., Mutanga, O., Sibanda, M., & Odindi, J. 2021. Estimating and monitoring land surface phenology in Rangelands: A review of progress and challenges. Remote Sensing, 13:11, 2060. https://doi.org/10.3390/rs13112060

Maynard, C. L., Lawrence, R. L., Nielson, G. A., & Decker, G. 2007. Ecological site descriptions and remotely sensed imagery as a tool for rangeland evaluation. Canadian Journal of Remote Sensing, 33, 109–115.

McCord, S. E., Buenemann, M., Karl, J. W., Browning, D. M., & Hadley, B. C. 2017. Integrating remotely sensed imagery and existing multiscale field data to derive Rangeland indicators: Application of Bayesian additive regression trees. Rangeland Ecology & Management, 70:5, 644–655, ISSN 1550–7424, https://doi.org/10.1016/j.rama.2017.02.004. (www.sciencedirect.com/science/article/pii/S1550742417300222)

McKeon, G. M., Stone, G. S., Syktus, J. I., Carter, J. O., Flood, N. R., Ahrens, D. G., Bruget, D. N., Chilcoty, C. R., Cobon, D. H., Cowley, R. A., Crimp, S. J., Fraser, G. W., Howden, S. M., Johnson, P. W., Ryan, J. G., Stokes, C. J., & Day, K. A. 2009. Climate change impacts on northern Australian rangeland livestock carrying capacity: A review of issues. Rangeland Journal, 31, 1–29.

McNairn, H., & Protz, R. 1993. Mapping corn residue cover on agricultural fields in Oxford County, Ontario, using Thematic Mapper. Canadian Journal of Remote Sensing, 19:152, 159.

Miao, X., Gong, P., Swope, S., Pu, R., Carruthers, R., & Anderson, G. L. 2007. Detection of yellow starthistle through band selection and feature extraction from hyperspectral imagery. Photogrammetric Engineering & Remote Sensing, 73, 1005–1015.

Miao, X., Gong, P., Swope, S., Pu, R., Carruthers, R., Anderson, G. L., Heaton, J. S., & Tracy, C. R. 2006. Estimation of yellow starthistle abundance through CASI-2 hyperspectral imagery using linear spectral mixture models. Remote Sensing of Environment, 101, 329–341.

Miao, X., Patil, R., Heaton, J. S., & Tracy, R. C. 2011. Detection and classification of invasive saltcedar through high spatial resolution airborne hyperspectral imagery. International Journal of Remote Sensing, 32, 2131–2150.

Mirik, M., Ansley, R. J., Steddom, K., Jones, D. C., Rush, C. M., Michels Jr., G. J., & Elliot, N. C. 2013. Remote distinction of a noxious weed (musk thistle: *Carduss nutans*) using airborne hyperspectral imagery and the support vector machine classifier. Remote Sensing, 5, 612–630.

Mirik, M., Steddom, K., & Michels Jr., G. J. 2006. Estimating biophysical characteristics of musk thistle (*Carduus nutans*) with three remote sensing instruments. Rangeland Ecology & Management, 59, 44–54.

Mitchell, J. J., & Glenn, N. F. 2009. Subpixel abundance estimates in mixture-tuned matched filtering classifications of leafy spurge (*Euphorbia esula* L.). International Journal of Remote Sensing, 30, 6099–6119.

Mladinich, C. S., Ruiz Bustos, M., Stitt, S., Root, R., Brown, K., Anderson, G. L., & Hager, S. 2006. The use of Landsat 7 Enhanced Thematic Mapper Plus for mapping leafy spurge. Rangeland Ecology & Management, 59, 500–506.

Moffet, C. A. 2009. Agreement between measurements of shrub cover using ground-based methods and very large scale aerial imagery. Rangeland Ecology & Management, 62, 268–277.

Montandon, L. M., & Small, E. E. 2008. The impact of soil reflectance on the quantification of the green vegetation fraction from NDVI. Remote Sensing of Environment, 112, 1835–1845.

Morgan, J. A., Milchunas, D. G., LeCain, D. R., West, M., & Mosier, A. R. 2007. Carbon dioxide enrichment alters plant community structure and accelerates shrub growth in the shortgrass steppe. Proceedings of the National Academy of Sciences, 104, 14724–14729.

Morisette, J. T., Jarnevich, C. S., Ullah, A., Cai, W., Pedelty, J. A., Gentle, J. E., Stohlgren, T. J., & Schnase, J. L. 2006. A tamarisk habitat suitability map for the continental United States. Frontiers of Ecology and Management, 4, 11–17.

Moseley, K., Shaver, P. L., Sanchez, H., & Bestelmeyer, B. T. 2010. Ecological site development: A gentle introduction. Rangelands, 32:6, 16–22.

Müllerová, J., Pergl, J., & Pyšek, P. 2013. Remote sensing as a tool for monitoring plant invasions: Testing the effects of data resolution and image classification approach on the detection of a model plant species *Heracleum mantegazzianum* (giant hogweed). International Journal of Applied Earth Observation and Geoinformation, 25, 55–65.

Mundt, J. T., Glenn, N. F., Weber, K. T., Prather, T. S., Lass, L. W., & Pettingill, J. 2005. Discrimination of hoary cress and determination of its detection limits via hyperspectral image processing and accuracy assessment techniques. Remote Sensing of Environment, 96, 509–517.

Nagler, P. L., Glenn, E. P., Jarnevich, C. S., & Shafroth, P. B. 2011. Distribution and abundance of saltcedar and Russian olive in the Western United States. Critical Reviews of Plant Science, 30, 508–523.

Nagler, P. L., Inoue, Y., Glenn, E. P., Russ, A. L., & Daughtry, C. S. T. 2003. Cellulose absorption index (CAI) to quantify mixed soil-plant litter scenes. Remote Sensing of Environment, 87, 310–325.

Narumalani, S., Mishra, D. R., Burkholder, J., Merani, P. B. T., & Wilson, G. 2006. A comparative evaluation of ISODATA and Spectral Angle Mapping for the detection of saltcedar using airborne hyperspectral imagery. Geocarto International, 21, 59–66.

Narumalani, S., Mishra, D. R., Wilson, R., Reece, P., & Kohler, A. 2009. Detecting and mapping four invasive species along the floodplain of North Platte River, Nebraska. Weed Technology, 23, 99–107.

National Research Council (NRC). 1994. *Rangeland Health, New Methods to Classify, Inventory, and Monitor Rangelands*. Washington, DC: National Academy Press, 180 pp.

Noujdina, N. V., & Ustin, S. L. 2008. Mapping downy brome (*Bromus tectorum*) using multidate AVIRIS data. Weed Science, 56, 173–179.

Ocholla, I. A., Pellikka, P., Karanja, F. N., Vuorinne, I., Odipo, V., & Heiskanen, J. 2024. Livestock detection in African rangelands: Potential of high-resolution remote sensing data. Remote Sensing Applications: Society and Environment, 33, 101139, ISSN 2352–9385, https://doi.org/10.1016/j.rsase.2024.101139. (www.sciencedirect.com/science/article/pii/S235293852400003X)

Oliver, I., Eldridge, D. J., Nadolny, C., & Martin, W. K. 2014. What do site condition multi-metrics tell us about species biodiversity? Ecological Indicators, 38, 262–271.

Olofsson, P., Foody, G. M., Stehman, S. V., & Woodcock, C. E. 2013. Making better use of accuracy data in land change studies: Estimating accuracy and area and quantifying uncertainty using stratified estimation. Remote Sensing of Environment, 129, 122–131.

Olsson, A. D., & Morisette, J. T. 2014. Comparison of simulated HyspIRI with two multispectral sensors for invasive species mapping. Photogrammetric Engineering & Remote Sensing, 80, 217–227.

O'Neill, M., Ustin, S. L., Hager, S., & Root, R. 2000. Mapping the distribution of leafy spurge at Theodore Roosevelt National Park using AVIRIS. In *Proceedings of the 10th AVIRIS Airborne Geoscience Workshop* (R. O. Green, ed.). Pasadena, CA: Jet Propulsion Laboratory.

Parker Williams, A. E., & Hunt Jr., E. R. 2002. Estimation of leafy spurge cover from hyperspectral imagery using mixture tuned matched filtering. Remote Sensing of Environment, 82, 446–456.

Parker Williams, A. E., & Hunt Jr., E. R. 2004. Accuracy assessment for detection of leafy spurge with hyperspectral imagery. Journal of Range Management, 57, 106–112.

Parkes, D., Newell, G., & Cheal, D. 2003. Assessing the quality of native vegetation: The 'habitat hectares' approach. Ecological Management & Restoration, 4(suppl), S29–S38.

Parracciani, C., Gigante, D., Mutanga, O., Bonafoni, S. & Vizzari, M. 2024. Land cover changes in grassland landscapes: Combining enhanced Landsat data composition, LandTrendr, and machine learning classification in google earth engine with MLP-ANN scenario forecasting. GIScience & Remote Sensing, 61:1, DOI: 10.1080/15481603.2024.2302221

Pellant, M., Shaver, P., Pyke, D. A., & Herrick, J. E. 2005. *Interpreting Indicators of Rangeland Health, Version 4.* Technical Reference 1734–6. Denver, CO: United States Department of Interior, Bureau of Land Management, 122 pp.

Pereira, H. M., Leadley, P. W., Proença, V., Alkemade, R., Scharlemann, J. P. W., Fernandez-Manjarrés, J. F., Araújo, M. G., Balvanera, P., Biggs, R., Cheung, W. W. L., Chini, L., Cooper, H. D., Gilman, E. L., Guénette, S., Hurtt, G. C., Huntington, H. P., Mace, G. M., Oberdorff, T., Revenga, C., Rodrigues, P., Scholes, R. J., Sumaila, U. R., & Walpole, M. 2010. Scenarios for global biodiversity in the 21st Century. Science, 330, 1496–1501.

Pereira, H. M., Navarro, L. M., & Martins, I. S. 2012. Global biodiversity change: The bad, the good, and the unknown. Annual Review of Environment and Resources, 37, 25–50.

Peters, A. J., Eve, M. D., Holt, E. H., & Whitford, W. G. 1997. Analysis of desert plant community growth patterns with high temporal resolution satellite spectra. Journal of Applied Ecology, 34, 418–432.

Peters, A. J., Reed, B. C., Eve, M. D., & McDaniel, K. C. 1992. Remote sensing of broom snakeweed (*Gutierrezia sarothrae*) with NOAA-10 spectral image processing. Weed Technology, 6, 1015–1020.

Peterson, A. T. 2003. Predicting the geography of species' invasions via ecological niche modeling. Quarterly Review of Biology, 78, 419–433.

Peterson, D. L., Price, K. P., & Martinko, E. A. 2002. Discriminating between cool season and warm season grassland cover types in northeastern Kansas. International Journal of Remote Sensing, 23, 5015–5030.

Pettorelli, N., Ryan, S., Mueller, T., Bunnefeld, N., Jędrejewska, B., Lima, M., & Kausrud, K. 2011. The normalized difference vegetation index (NDVI): Unforeseen successes in animal ecology. Climate Research, 46, 15–27.

Polley, H. W., Briske, D. D., Morgan, J. A., Wolter, K., Bailey, D. W., & Brown, J. R. 2013. Climate change and North American Rangelands: Trends, projections, and implications. Rangeland Ecology & Management, 66, 493–511.

Pu, R. 2008. Invasive species change detection using artificial neural networks and CASI hyperspectral imagery. *Environmental Monitoring and Assessment*, 140, 15–32.

Pu, R. 2012. Detecting and mapping invasive plant species by using hyperspectral data. Pages 447–465 in *Hyperspectral Remote Sensing of Vegetation* (P. S. Thenkabail, J. G. Lyon and A. Huete, eds.). Boca Raton, FL: CRC Press-Taylor Francis Group.

Pu, R., Gong, P., Tian, Y., Miao, X., Carruthers, R. I., & Anderson, G. L. 2008. Using classification and NDVI differences for monitoring sparse vegetation coverage: A case study of saltcedar in Nevada, USA. International Journal of Remote Sensing, 29, 3987–4011.

Pyke, D. A., Herrick, J. E., Shaver, P., & Pellant, M. 2002. Rangeland health attributes and indicators for qualitative assessment. Journal of Range Management, 55, 584–597.

Questad, E. J., Antill, M., Liu, N., Natasha Stavros, E., Townsend, P. A., Bonfield, S., & Schimel, D. 2022. A camera-based method for collecting rapid vegetation data to support remote-sensing studies of Shrubland biodiversity. Remote Sensing, 14:8, 1933. https://doi.org/10.3390/rs14081933

Quilter, M. C., & Anderson, V. J. 2000. Low altitude/large scale aerial photographs: A tool for range and resource managers. Rangelands, 22:2, 13–17.

Quilter, M. C., & Anderson, V. J. 2001. A proposed method for determining shrub utilization using (LA/LS) imagery. Journal of Range Management, 54, 378–381.

Ramoelo, A., Skidmore, A. K., Cho, M. A., Schlerf, M., Mathieu, R., & Heitkönig, I. M. A. 2012. Regional estimation of savanna grass nitrogen using the red-edge band of the spaceborne RapidEye sensor. International Journal of Applied Earth Observation and Geoinformation, 19, 151–162.

Ramoelo, A., Skidmore, A. K., Schlerf, M., Mathieu, R., & Heitkönig, I. 2011. Water-removed spectra increase the retrieval accuracy when estimating savanna grass nitrogen and phosphorus concentrations. ISPRS Journal of Photogrammetry and Remote Sensing, 66, 408–417.

Rango, A., Laliberte, A., Herrick, J. E., Winters, C., Havstad, K., Steele, C., & Browning, D. 2009. Unmanned aerial vehicle-based remote sensing for rangeland assessment, monitoring and management. Journal of Applied Remote Sensing, 3, 033542.

Rango, A., Laliberte, A., Steele, C., Herrick, J. E., Bestelmeyer, B., Schmugge, T., Roanhorse, A., & Jenkins, V. 2006. Using unmanned aerial vehicles for rangelands: Current applications and future potentials. Environmental Practice, 8, 159–168.

Reed, B. C., Brown, J. F., VanderZee, D., Loveland, T. R., Merchant, J. W., & Ohlen, D. O. 1994. Measuring phenological variability from satellite imagery. Journal of Vegetation Science, 5, 703–714.

Reeves, M. C., Angerer, J., Hunt, E. R., Kulawardhana, W., Kumar, L., Loboda, T., Loveland, T., Metternicht, G., Ramsey, R. D., & Washington-Allen, R. A. In press. A global view of remote sensing of rangelands: Evolution, applications, and future pathways. Chapter 10 in *Remote Sensing Handbook. Volume II: Land Resources: Monitoring, Modeling, and Mapping* (P. S. Thenkabail, ed.). Boca Raton, FL: CRC Press Taylor & Francis Group.

Reich, P. B., Tilman, D., Isbell, F., Mueller, K., Hobbie, S. E., Flynn, D. F. B., & Eisenhauer, N. 2012. Impacts of biodiversity loss escalate through time as redundancy fades. Science, 336, 587–592.

Retallack, A., Finlayson, G., Ostendorf, B., Clarke, K., & Lewis, M. 2023. Remote sensing for monitoring rangeland condition: Current status and development of methods. Environmental and Sustainability Indicators, 19, 100285, ISSN 2665–9727, https://doi.org/10.1016/j.indic.2023.100285. (www.sciencedirect.com/science/article/pii/S2665972723000624)

Ricotta, C., Reed, B. C., & Tieszen, L. T. 2003. The role of C_3 and C_4 grasses to interannual variability in remotely sensed ecosystem performance over the US Great Plains. International Journal of Remote Sensing, 24, 4421–4431.

Roberts, D. A., Quattrochi, D. A., Hulley, G. C., Hook, S. J., & Green, R. O. 2012. Synergies between VSWIR and TIR data for the urban environment: An evaluation of the potential for the Hyperspectral Infrared Imager (HyspIRI) Decadal Survey mission. Remote Sensing of Environment, 117, 83–101.

Roberts, D. A., Smith, M. O., & Adams, J. B. 1993. Green vegetation, nonphotosynthetic vegetation, and soils in AVIRIS data. Remote Sensing of Environment, 44, 255–269.

Rocchini, D., Balkenhol, N., Carter, G. A., Foody, G. M., Gillespie, T. W., He, K. S., Kark, S., Levin, N., Lucas, K., Luoto, M., Nagendra, H., Oldeland, J., Ricotta, C., Southworth, J., & Neteler, M. 2010a. Remotely sensed spectral heterogeneity as a proxy of species diversity: Recent advances and open challenges. Ecological Informatics, 5, 318–329.

Rocchini, D., He, K. S., Oldeland, J., Wesuls, D., & Neteler, M. 2010b. Spectral variation versus species β-diversity at different spatial scales: A test in African highland savannas. Journal of Environmental Monitoring, 12, 825–831.

Rouse, J. W., Haas, R. H., Schell, J. A., & Deering, D. W. 1974. Monitoring vegetation systems in the Great Plains with ERTS. Pages 309–317 in *Third Earth Resources Technology Satellite-1Symposium, Volume 1: Technical Presentations*, NASA SP-351 (S. C. Freden, E. P. Mercanti and M. Becker, eds.). Washington, DC: National Aeronautics and Space Administration.

RSAC (Remote Sensing Applications Center). 2014. *Digital Mylar*. www.fs.fed.us/eng/rsac/digitalmylar/, last accessed 9 June 2014.

Running, S. W., Loveland, T. R., Pierce, L. L., Nemani, R., & Hunt Jr., E. R. 1995. A remote sensing based vegetation classification logic for global land cover analysis. Remote Sensing of Environment, 51, 39–48.

Sadler, R. J., Hazelton, M., Boer, M., & Grierson, P. F. 2010. Deriving state-and-transition models from an image series of grassland pattern dynamics. Ecological Modelling, 221, 433–444.

Sage, R. F., & Kubien, D. S. 2007. The temperature response of C_3 and C_4 photosynthesis. Plant, Cell & Environment, 30, 1086–1106.

Sampson, A. W. 1919. *Plant Succession Relation to Range Management*. USDA Technical Bulletin No. 791. Washington, DC: United States Department of Agriculture, 76 p.

Samuel, L. W., Kirby, D. R., Norland, J. E., & Anderson, G. L. 2008. Leafy spurge suppression by flea beetles in the Little Missouri Drainage Basin, USA. Rangeland Ecology & Management, 61, 437–443.

Savitzky, A., & Golay, M. J. E. 1964. Smoothing and differentiation of data by simplified least squares procedures. Analytical Chemistry, 36, 1627–1639.

Sawalhah, M. N., Al-Kofahi, S. D., Othman, Y. A., & Cibils, A. F. 2018. Assessing rangeland cover conversion in Jordan after the Arab spring using a remote sensing approach. Journal of Arid Environments, 157, 97–102, ISSN 0140–1963, https://doi.org/10.1016/j.jaridenv.2018.07.003. (www.sciencedirect.com/science/article/pii/S0140196318304415)

Schwartz, M. D., Reed, B. C., & White, M. A. 2002. Assessing satellite-derived start-of-season measures in the Conterminous USA. International Journal of Climate, 22, 1793–1805.

Serbin, G., Hunt Jr., E. R., Daughtry, C. S. T., & McCarty, G. W. 2013. Assessment of spectral indices for cover estimation of senescent vegetation. Remote Sensing Letters, 4, 552–560.

Serbin, G., Hunt Jr., E. R., Daughtry, C. S. T., McCarty, G. W., & Doraiswamy, P. C. 2009. An improved ASTER index for remote sensing of crop residue. Remote Sensing, 1, 971–991.

Shenk, J. S., Workman Jr., J. J., & Westerhaus, M. O. 2008. Application of NIR spectroscopy to agricultural products. Pages 347–386 in *Handbook of Near-Infrared Analysis, 3rd Edition* (D. A. Burns and E. W. Ciurczak, eds.). Boca Raton, FL: CRC Press.

Singh, N., & Glenn, N. F. 2009. Multitemporal spectral analysis for cheatgrass (*Bromus tectorum*) classification. International Journal of Remote Sensing, 30, 3441–3462.

Skidmore, A. K., Ferwerda, J. G., Mutanga, O., Van Wieren, S. E., Peel, M., Grant, R. C., Prins, H. H. T., Balcik, F. B., and Venus, V. 2010. Forage quality of savannas – simultaneously mapping foliar protein and polyphenols for trees and grass using hyperspectral imagery. Remote Sensing of Environment, 114, 64–72.

Soussanna, J.-F., & Lüscher, A. 2007. Temperate grasslands and global atmospheric change: A review. Grass and Forage Science, 62, 127–134.

Southard, G. 2013. A little UAV grows up. Presented on 27 March 2013 at the American Society of Photogrammetry and Remote Sensing 2013 Annual Conference, Baltimore, MD, USA.

Stafford Smith, D. M., McKeon, G. M., Watson, I. W., Henry, B. K., Stone, G. S., Hall, W. B., & Howden, S. M. 2007. Learning from episodes of degradation and recovery in variable Australian rangelands. Proceedings of the National Academy of Sciences, 104, 20690–20695.

Starks, P. J., Coleman, S. W., & Phillips, W. A. 2004. Determination of forage chemical composition using remote sensing. Rangeland Ecology & Management, 57, 635–640.

Steele, C. M., Bestelmeyer, B. T., Burkett, L. M., Smith, P. L., & Yanoff, S. 2012. Spatially explicit representation of state-and-transition models. Rangeland Ecology & Management, 65, 213–222.

Stitt, S., Root, R., Brown, K., Hager, S., Mladinich, C., Anderson, G. L., Dudek, K., Ruiz Bustos, M., & Kokaly, R. 2006. Classification of leafy spurge with Earth Observing-1 Advanced Land Imager. Rangeland Ecology & Management, 59, 507–511.

St-Louis, V., Pidgeon, A. M., Clayton, M. K., Locke, B. A., Bash, D., & Radeloff, V. C. 2009. Satellite image texture and a vegetation index predict avian biodiversity in the Chihuahuan desert of New Mexico. Ecography, 32, 468–480.

Stohlgren, T. J., Ma, P., Kumar, S., Rocca, M., Morisette, J. T., Jarnevich, C. S., & Benson, N. 2010. Ensemble habitat mapping of invasive plant species. Risk Analysis, 30, 224–235.

Tews, J., Brose, U., Grimm, V., Tielbörger, K., Wichmann, M. C., Schwager, M., & Jeltsch, F. 2004. Animal species diversity driven by habitat heterogeneity/diversity: The importance of keystone structures. Journal of Biogeography, 31, 79–92.

Thornley, R. H., Gerard, F. F., White, K., and Verhoef, A. 2023. Prediction of Grassland biodiversity using measures of spectral variance: A meta-analytical review. Remote Sensing, 15(3), 668. https://doi.org/10.3390/rs15030668

Thorp, K. R., French, A. N., & Rango, A. 2013. Effect of image spatial and spectral characteristics on mapping semi-arid rangeland vegetation using multiple endmember spectral mixture analysis (MESMA). Remote Sensing of Environment, 132, 120–130.

Thuiller, W., Richardson, D. M., Pyšek, P., Midgley, G. F., Hughes, G. O., & Rouget, M. 2005. Niche-based modeling as a tool for predicting the risk of alien plant invasions at a global scale. Global Change Biology, 11, 2234–2250.

Tieszen, L. L., Reed, B. C., Bliss, N. B., Wylie, B. K., & DeJong, D. D. 1997. NDVI, C_3 and C_4 production and distributions in Great Plains grassland land cover classes. Ecological Applications, 7, 59–78.

Tilman, D., Reich, P. B., & Isbell, F. 2012. Biodiversity impacts ecosystem productivity as much as resources, disturbance, or herbivory. Proceedings of the National Academy of Sciences, 109, 10394–10397.

Tilman, D., Reich, P. B., & Knops, J. M. H. 2006. Biodiversity and ecosystem stability in a decade-long grassland experiment. Nature, 441, 629–632.

Tomlins, G. F., & Lee, Y. J. 1983. Remotely piloted aircraft—an inexpensive option for large-scale aerial photography in forestry applications. Canadian Journal of Remote Sensing, 9, 76–85.

Townshend, J. R. G., & Justice, C. O. 1988. Selecting the spatial resolution of satellite sensors required for global monitoring of land transformations. International Journal of Remote Sensing, 9, 187–236.

Trimble Navigation Limited. 2013. *Trimble Unmanned Aircraft Systems for Surveying and Mapping*. Westminster, CO: Trimble Navigation Limited. www.trimble.com/Survey/unmanned-aircraft-systems.aspx, last accessed 9 June 2014.

Tucker, C. J. 1979. Red and photographic infrared linear combinations for monitoring vegetation. Remote Sensing of Environment, 8, 127–150.

Turner, D., Lucieer, A., & Watson, C. 2012. An automated technique for generating georectified mosaics from ultra-high resolution unmanned aerial vehicle (UAV) imagery, based on structure from motion (StM) point clouds. Remote Sensing, 4, 1392–1410.

Underwood, E. C., Klinger, R., & Moore, P. E. 2004. Predicting patterns of non-native plant invasions in Yosemite National Park, California, USA. Diversity and Distributions, 10, 447–459.

Underwood, E. C., Ustin, S., & DiPietro, D. 2003. Mapping nonnative plants using hyperspectral imagery. Remote Sensing of Environment, 86, 150–161.

Underwood, E. C., Ustin, S. L., & Ramirez, C. M. 2007. A comparison of spatial and spectral image resolution for mapping invasive plants in coastal California. Environmental Management, 39, 63–83.

USDA NRCS. 2006. United States Department of Agriculture, Natural Resource Conservation Service. *Land Resource Regions and Major Land Resource Areas of the United States, the Caribbean, and the Pacific Basin*. Handbook 206. Washington, DC: United States Department of Agriculture. www.nrcs.usda.gov/wps/portal/nrcs/detail/soils/survey/?cid=nrcs142p2_053624, last accessed 28 Feb. 2014.

Ustin, S. L., & Gamon, J. A. 2010. Remote sensing of plant functional types. New Phytologist, 186, 795–816.

Ustin, S. L., Riaño, D., & Hunt Jr., E. R. 2012. Estimating canopy water content from spectroscopy. Israel Journal of Plant Science, 60, 9–23.

Ustin, S. L., Valko, P. G., Kefauver, S. C., Santos, M. J., Zimpfer, J. F., & Smith, S. D. 2009. Remote sensing of biological soil crust under simulated climate change manipulations in the Mojave Desert. Remote Sensing of Environment, 113, 317–328.

van der Meer, F. 2006. The effectiveness of spectral similarity measures for the analysis of hyperspectral imagery. International Journal of Applied Earth Observation and Geoinformation, 8, 3–17.

van Deventer, A. P., Ward, A. D., Gowda, P. H., & Lyon, J. G. 1997. Using thematic mapper data to identify contrasting soil plains to tillage practices. Photogrammetric Engineering & Remote Sensing, 63, 87–93.

Vrieling, A., Rodrigues, S. C., Bartholomeus, H., & Sterk, G. 2007. Automatic identification of erosion gullies with ASTER imagery in the Brazilian Cerrados. International Journal of Remote Sensing, 28, 2723–2738.

Wang, C., Bentivegna. D. J., Smeda, R. J., & Swanigan, R. E. 2010a. Comparing classification approaches for mapping cut-leaved teasel in highway environments. *Photogrammetric Engineering & Remote Sensing*, 76, 567–575.

Wang, C., Fritschi, F. B., Stacey, G., & Yang, Z. 2011a. Phenology-based assessment of perennial energy crops in North American Tallgrass Prairie. Annals of the Association of American Geographers, 101, 741–751.

Wang, C., Hunt Jr., E. R., Zhang, L., & Guo, H. 2013. Spatial distributions of C_3 and C_4 grass functional types in the U.S. Great Plains and their dependency on inter-annual climate variability. Remote Sensing of Environment, 128, 90–101.

Wang, C., Jamison, B. E., & Spicci, A. A. 2010b. Trajectory-based warm season grassland mapping in Missouri prairies with multi-temporal ASTER imagery. Remote Sensing of Environment, 114, 531–539.

Wang, C., Zhou, B., & Palm, H. L. 2008. Detecting invasive sericea lespedeza (*Lespedeza cuneata*) in Mid-Missouri pastureland using hyperspectral imagery. Environmental Management, 41, 853–862.

Wang, K., Franklin, S. E., Guo, X., & Cattet, M. 2010c. Remote sensing of ecology, biodiversity and conservation: A review from the perspective of remote sensing specialists. Sensors, 10, 9647–9667.

Wang, L., Hunt Jr., E. R., Qu, J., Hao, X., & Daughtry, C. S. T. 2011b. Estimating dry matter content of fresh leaves from the residuals between leaf and water reflectance. Remote Sensing Letters, 2, 137–145.

Ward, D. P., & Kutt, A. S. 2009. Rangeland biodiversity assessment using fine scale on-ground survey, time series of remotely sensed ground cover and climate data: An Australian savanna case study. Landscape Ecology, 24, 495–507.

Washington-Allen, R. A., Van Niel, T. G., Ramsey, R. D., & West, N. E. 2004. Remote sensing-based piosphere analysis. GIScience & Remote Sensing, 41, 136–154.

Washington-Allen, R. A., West, N. E., Ramsey, R. D., & Efromson, R. A. 2006. A protocol for retrospective remote sensing-based ecological monitoring of rangelands. Rangeland Ecology & Management, 59, 19–29.

Watts, A. C., Ambrosia, V. G., & Hinckley, E. A. 2012. Unmanned aircraft systems in remote sensing and scientific research: Classification and considerations of use. Remote Sensing, 4, 1671–1692.

Weber, B., Olehowski, C., Knerr, T., Hill, J., Deutschewitz, K., Wessels, D. C. J., Eitel, B., & Büdel, B. 2008. A new approach for mapping of biological soil crusts in semidesert areas with hyperspectral imagery. Remote Sensing of Environment, 112, 2187–2201.

Weber, K. T., Chen, F., Booth, D. T., Raza, M., Serr, K., & Gokhale, B. 2013. Comparing two ground-cover measurement methodologies for semiarid rangelands. Rangeland Ecology & Management, 66, 82–87.

Westoby, M. J., Brasington, J., Glasser, N. F., Hambrey, M. J., & Reynolds, J. M. 2012. 'Structure-from-Motion' photogrammetry: A low-cost, effective tool for geosciences applications. Geomorphology, 179, 300–314.

Williamson, J. C., Bestelmeyer, B. T., & Peters, D. P. C. 2012. Spatiotemporal patterns of production can be used to detect state change across an arid landscape. Ecosystems, 15, 34–47.

Winslow, J. C., Hunt Jr., E. R., & Piper, S. C. 2003. The influence of seasonal water availability on global C_3 vs C_4 grassland biomass and its implications for climate change research. Ecological Modelling, 163, 153–173.

Wood, E. M., Pidgeon, A. M., Radeloff, V. C., & Keuler, N. S. 2012. Image texture as a remotely sensed measure of vegetation structure. Remote Sensing of Environment, 121, 516–526.

Wood, E. M., Pidgeon, A. M., Radeloff, V. C., & Keuler, N. S. 2013. Image texture predicts avian density and species richness. PLoS-One, 8, e63211.

Yang, C., & Everitt, J. H. 2010a. Comparison of hyperspectral imagery with aerial photography and multispectral imagery for mapping broom snakeweed. International Journal of Remote Sensing, 31, 5423–5438.

Yang, C., & Everitt, J. H. 2010b. Mapping three invasive weeds using airborne hyperspectral imagery. Ecological Informatics, 5, 429–439.

Yang, C., Everitt, J. H., & Fletcher, R. S. 2013. Evaluating airborne hyperspectral imagery for mapping saltcedar infestations in west Texas. Journal of Applied Remote Sensing, 7, 073556–1.

Yang, C., Everitt, J. H., and Johnson, H. B. 2009. Applying image transformation and classification techniques to airborne hyperspectral imagery for mapping Ashe juniper infestations. International Journal of Remote Sensing, 30, 2741–2758.

Yu, Q., Gong, P., Clinton, N., Biging, G., Kelly, M., & Schirokauer, D. 2006. Object-based detailed vegetation classification with airborne high spatial resolution remote sensing imagery. Photogrammetric Engineering & Remote Sensing, 72, 799–811.

Zavaleta, E. S., Pasari, J. R., Hulvey, K. B., & Tilman, G. D. 2010. Sustaining multiple ecosystem functions in grassland communities requires higher biodiversity. Proceedings of the National Academy of Sciences, 107, 1443–1446.

Zengeya, F. M., Mutanga, O., and Murwira, A. 2013. Linking remotely sensed forage quality estimates from WorldView-2 multispectral data with cattle distribution in a savanna landscape. International Journal of Applied Earth Observation and Geoinformation, 21, 513–524.

Zhang, X., Friedl, M. A., Schaaf, C. B., Strahler, A. H., Hodges, J. C. F., Gao, F., Reed, B. C., & Huete, A. 2003. Monitoring vegetation phenology using MODIS. Remote Sensing of Environment, 84, 471–75.

Ziska, L. H., Blumenthal, D. M., Runion, G. B., Hunt Jr., E. R., & Diaz-Soltero, H. 2011. Invasive species and climate change: An agronomic perspective. Climatic Change, 105, 13–42.